Journal Pre-proof

Destinations frequently impacted by dust storms originating from southwest Iran

Parya Broomandi, Ferhat Karaca, Mert Guney, Aram Fathian, Xueyu Geng, Jong Ryeol Kim

PII: S0169-8095(20)31201-1

DOI: https://doi.org/10.1016/j.atmosres.2020.105264

Reference: ATMOS 105264

To appear in: *Atmospheric Research*

Received date: 9 April 2020

Revised date: 12 September 2020

Accepted date: 12 September 2020

Please cite this article as: P. Broomandi, F. Karaca, M. Guney, et al., Destinations frequently impacted by dust storms originating from southwest Iran, *Atmospheric Research* (2020), https://doi.org/10.1016/j.atmosres.2020.105264

Destinations Frequently Impacted by Dust Storms Originating from Southwest Iran

Parya Broomandi [1,2,3], Ferhat Karaca [1,4], Mert Guney [1,4], Aram Fathian [5], Xueyu Geng [2], Jong Ryeol Kim [1*]

[1] Department of Civil and Environmental Engineering, Nazarbayev University 010000 Nur-Sultan, Kazakhstan

[2] Geotechnical Engineering, School of Engineering, The University of Warwick, CV4 7AL Coventry, UK

[3] Department of Chemical Engineering, Masjed-Soleiman Branch, Islamic Azad University, Masjed-Soleiman, Iran

[4] The Environment & Resource Efficiency Cluster (EREC), Nazarbayev University 010000 Nur-Sultan, Kazakhstan

[5] Neotectonics and Natural Hazards Institute, RWTH Aachen University, Aachen, Germany

* Corresponding author. Email: jong.kim@nu.edu.kz, Phone: +7 7172 70 9136, and Fax: +7 7172 70 9136.

Destinations Frequently Impacted by Dust Storms Originating from Southwest Iran

Abstract

Deserts can be considered as one of the main sources of dust emissions as they are highly vulnerable to wind erosion, i.e. The lack of vegetative cover, as well as low soil wetness, contribute to the release of particles by wind erosion. The present study examines the seasonal variation in sand and dust storms (SDSs) originating from war-impacted semi-arid bare lands affected by chemical warfare located in southwest Iran for the period of 2007-2018. It employs a synthesis of satellite observations and Hybrid Single-Particle Lagrangian Integrated Trajectory (HYSPLIT) model trajectories. A regression analysis between annual/seasonal absorbing aerosol index distribution and selected parameters indicated strong correlation with surface skin temperature, topsoil layer wetness, and 10-m wind speed. During both cold and warm periods, Kuwait and the Persian Gulf were highly vulnerable to episodic dust incursions as they were identified in the maximum impact zone (frequency of 100%). The Persian Gulf was affected by about 12% of the total air masses during the warm period, which increased to 74% during the cold period. Regarding the vulnerability to the high wind of war-impacted regions presumably contaminated with potentially toxic elements (PTEs) and toxic compounds, the particles of contaminated dust may have been continuously transported over by the strong winds not only the surrounding region but also long distances including agricultural land and marine environment. The study area would possibly pose a danger to the environment and human health; therefore, a detailed site characterization to investigate the degree of contamination with PTEs and toxic compounds is warranted.

Keywords: Absorbing aerosol index (AAI); Air pollution modelling; Particulate matter; Sand and dust storms (SDS); The Persian Gulf

1. Introduction

Regional and long-range transportation of mineral dust is an essential component of the atmospheric circulation. It is caused by wind erosion and transported from a local scale to a global scale by air systems. Sand and dust storms (SDSs), which are the significant sources of airborne dust, are recognized as common phenomena originating from global deserts, and they cause serious adverse human health, climate, environmental, and economic impacts (Ginoux, et al., 2012; Goudie, 2014). Accordingly, research on sand and dust cycles and routes are needed for specific issues concerning human health, weather, climate change, ecosystems, and air quality.

The primary SDS origins over the globe are located around arid regions, which are typically found on alluvial sedimentation basins at lower elevations with annual precipitation <200 mm, and with limited vegetation cover (Ginoux et al., 2012; Prospero et al., 2002). The most generative areas are detected in the north of Aral and Turkmenistan basins, the southern and eastern parts of Arabian Peninsula, the Syria-Iraqi desert, the Oman desert, and some closed inland areas of the Iranian plateau (such as Sistan Basin, Hamoun Jaz-Mourian Lake, Kavir and Lut deserts). The Middle East region and the Arabian Peninsula are responsible for releasing significant amounts of dust mainly transported over the Arabian Sea with substantial intensity from June to August (Prijith et al., 2013). Previous studies also showed that about 65% of the southwest Asian arid terrain has the potential to become a dust origin (Ginoux et al., 2012; Prospero et al., 2002). Although the Thar, Iraqi, and Arabian deserts are primary dust origins in South Asia, a small area (Sistan basin) with dried lakes (Hamoun) at the Iran-Afghanistan borders may also have a significant role (Karimi et al., 2012; Maghrabi et al., 2011; Prospero et al., 2002; Rashki et al., 2015, 2013). Furthermore, researchers showed the southwest Iran (Khuzestan Province) turning into one of the significant sand and

dust sources in the region (Broomandi et al., 2018, 2017a; Cao et al., 2015; Esmaili et al., 2006; Salmabadi et al., 2020).

Excessive dust loading over South Asia impacts the regional environment (terrestrial and marine) as well as the climate. It can easily alter the radiative forcing of the atmosphere and the biogeochemical cycles. Dust plumes can impact weather by affecting the hydrological cycle and cloud microphysics (Dipu et al., 2013), and influence the atmospheric thermal structure by suppressing cyclone activity (Dunion and Velden, 2002; Lemaitre et al., 2010). Studies also confirmed the impact of dust originating from southwest Asia and the Middle East on the acceleration of western Himalayas glacier melting (Prasad et al., 2009). Jickells et al. (2005) estimated the amount of global dust deposition to the oceans be about 450 $Tg.a^{-1}$, among which about 21% settles into the Pacific Ocean, 25% into the Indian Ocean and 47% settles into the Atlantic Ocean (Jickells et al., 2005; Wang et al., 2017).

By adding dissolved iron (Fe) to marine ecosystems, deposited dust aerosols can impact marine productivity (Kessler et al., 2019; Ueda et al., 2020; Wang et al., 2017). The amount of absorbed CO_2 by oceans can be altered by dissolved iron, which indirectly causes climate change. As a result, climate change can affect dust origin, emission fluxes, transport, and deposition processes. Worldwide, in most marine environments, dust aerosols (coming from major deserts) are responsible for the Fe input to the ocean surface (Kessler et al., 2019; Wang et al., 2017). Desert dust is a complex matrix of minerals, with variable structure, size, and Fe content. Beside Fe content, multiple factors control the rate of Fe release from dust minerals such as weathering degree, mineral structure, size, and occurring reactions during transport (in the atmosphere) and deposition (in the ocean microlayer) (Kessler et al., 2019). Fe is an essential nutrient element for all living organisms and acts as a limiting factor in the growth of marine plankton (Wang et al., 2017).

Also, Rashki et al. (2015) pointed out some supporting evidence that the Sistan dust storms influence some parts of the Arabian Sea, controlling the aerosol optical depth evolution over the marine environment. Dust deposition over the Arabian Sea can cool the ocean surface, influence the phytoplankton, and affect the chlorophyll blooming (Rashki et al., 2015; Singh et al., 2008). Likewise, mineral dust has been suspected to be one of the most critical health risk factors for pulmonary diseases including asthma and allergies in young as well as older adults and contributes to meningitis in Sistan province of Iran (Goudarzi et al., 2018; Merrifield et al., 2013; Miri et al., 2007; Mohammadi et al., 2015; Naimabadi et al., 2016) and in West Africa (Martiny and Chiapello, 2013). While fossil fuel combustion, traffic emissions, upwind petroleum industry, and gas and oil drilling activities are the primary contributing anthropogenic sources in the Middle East, the war remains can be added to the list for southwest Iran, Iraq, and Syria. There exist some previous studies examining the SDS storms originating from southwest Iran (Shalamcheh region, (30° 45'N and 48° 15'E)), which is a war-impacted SDS source area (Broomandi et al., 2018, 2017a). One of the critical anthropogenic origins of enriched trace elements in this area attributed to the remains of the Iraq-Iran war (Broomandi et al., 2017). For example, the high levels of Cl and S in this area were attributed to the use of mustard gas in Iraq- Iran war during 1980–1988, and Br, Mo, Zn, and Hg were other highly enriched trace elements detected in this war-impacted area (Broomandi et al., 2017a). The presence of Pb, Cu, Hg, Br, Mo, and Zn in contaminated soils has previously been attributed to war activities (Wallace, 2018). Due to a higher level of health risk exposure, The Hg contamination in the Shalamcheh region represents a significant concern as it could be washed out by atmospheric precipitation, potentially leading to regional underground water contamination (Broomandi et al., 2017a; Wallace, 2018).

A long-term analysis of the occurrence of dust storms still lacks over southwest Asia, including the Shalamcheh region, due to the limitations of satellite imagery at the regional

scale (Rashki et al., 2015). The identification of SDS pathways and origins uses specific techniques including satellite remote sensing, ground-based observations, trajectory analysis, and integrated approaches (Ashrafi et al., 2014; Broomandi et al., 2018; Rashki et al., 2015; Shao et al., 2011; Sorek-Hamer et al., 2013) and it is a significant challenge to perform in some areas of the Middle East due to certain limitations including the reliability and availability of data. Recently, the development of Global Dust Detection Index (GDDI) model (Karimi et al., 2012) and the new Middle East Dust Index (MEDI) had a significant contribution in the identification of SDS sources in the Middle East (Samadi et al., 2014). The employment of the satellite images for monitoring SDS events is an appropriate method that is time-saving and cost-effective; however, some ground sensors with systematic xerography are needed in continuous monitoring of the surfaces covered by dust during storms (Ekhtesasi and Gohari, 2012). To the best of our knowledge, there exists no study examining the common dust transport pathways and impact zones over the region originated by the Shalamcheh during SDS events.

The current research aims to assess the seasonal formation (during the cold and warm periods) and the prevalence of SDSs originated from southwest Iran (Shalamcheh region) under specific metrological conditions (e.g., wind speeds >20 knots (kn, 1 kn = 1.852 $km.h^{-1}$), horizontal visibility <1000 m) during 2007-2018. By providing quantitative measures, it aims to conclude whether the region can be listed among potential global sources of SDS and further assesses the long-range transport pathways and possible deposition and exposure concentration impacts of identified SDSs over the area by identifying its impact zones.

2. Material and Methods

2.1. Study area

The study area, Shalamcheh, is in southwest Iran in Khuzestan province (30°45’ N and 48°15’ E) (Figure 1). The area is bare land that has been affected by chemical warfare, mainly mustard gas, during the Iraq-Iran War between 1980 and 1988 (Broomandi et al., 2017a). There are two seasons in the region; the warm period is from April to September, and the cold period is from October to March. During warm and cold periods, the average received rainfall values were 17.5 ± 1.9 mm and 130.2 ± 60.6 mm; the average maximum temperature values were 46.1 ± 1.1 °C and 30.3 ± 1.1 °C, and the average relative humidity values were 32.5 ± 4.8 %, and 62.0 ± 4.6 %, respectively (Broomandi et al., 2017a).

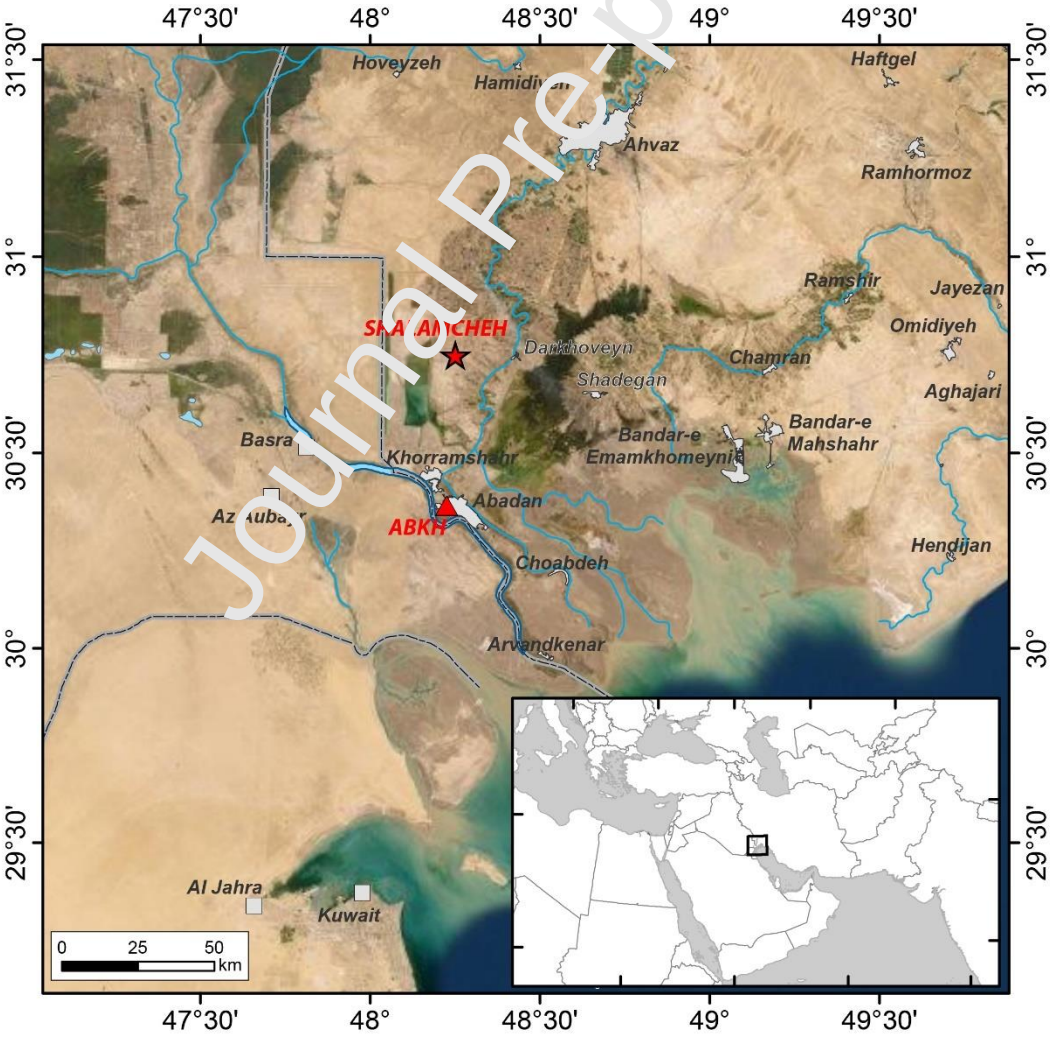

Figure 1. Location of study area, Shalamcheh, situated in Khuzestan Province of Southwest Iran. The solid red star indicates the study area (Shalamcheh). The solid red triangle represents the location of the Abadan and Khorramshahr meteorological station (ABKH).

2.2. Satellite data, trajectory, and dispersion modelling

Ozone Monitoring Instrument (OMI) absorbing aerosol index (AAI) database (http://giovanni.sci.gsfc.nasa.gov) was used (a) to evaluate the regional aerosol loads in the atmosphere and (b) to investigate the role of surface skin temperature and topsoil layer moisture in dust generation mechanism during 12 years (between 2007 and 2018). Monthly averaged AAI values at the spatial resolution of 1° × 1°, daily surface skin temperature (the mean temperature of earth's surface) at the spatial resolution of 0.25° × 0.25°, and topsoil layer moistures (the averaged value of water content in depth of 0-10 cm underground) at the spatial resolution of 0.5° × 0.625° were used. All meteorological parameters including wind speed and horizontal visibility were daily averaged (24 hour based measurements) and taken from Abadan and Khoramshahr metrological station (30°.21′N, 48°.13′E), which is the nearest station to the Shalamcheh (Ahvaz IRIMO, 2016).

The Hybrid Single-Particle Lagrangian Integrated Trajectory (HYSPLIT) model is for trajectory, dispersion, and deposition calculations employing the Global Forecast System (GFS) meteorological forecast parameters of the Global Data Assimilation System (GDAS) as its initial background field. Using particle or puff approaches, it calculates trajectories as well as dispersion and deposition simulations (Ashrafi et al., 2014; Lu et al., 2018). The trajectory computation in any Lagrangian model is based on the meteorological data (U, V, and W), which has been interpolated to the grids of the model.

The trajectory simulations in the present study were forwards and backwards moving from and to the dust source (30° 45' N and 48°15' E). They were run based on episodic events as suggested by de Villiers and van Heerden (2011) where a storm is classified either as sand and dust storm (e.g. 10-m wind speed >20 kn with visibility <1000 m) or severe sand and dust storm (e.g., the 10-m wind speed >30 kn with visibility <200 meters). The trajectories started at the height of one half of the mixed boundary layer. The height of mixing boundary layer and its mid-level were calculated by the HYSPLIT model and could be automatically selected using the method options (Draxler and Hess, 1997). Table 1 summarizes the monthly frequency of the identified sand and dust storms during the study period.

3. Results and Discussion

3.1. Sand and dust storm & severe sand and dust storm occurrences in Shalamcheh

The mean values for OMI AAI data were calculated from the daily absorbing aerosol index records for the study area. Typically, AAI values are ranging from a minimum of 0 to a maximum of 40 where higher numbers (e.g. >20) may indicate episodic atmospheric aerosol loads from dust storms or smoke emissions during the satellite scans. The daily average concentrations of absorbing aerosols are high during the warm period and especially in May, June, and July (with the highest value 27 in June); they can be attributed to mineral dust origins since no significant anthropogenic dust generation mechanisms are available in the region during the summertime. The average AAI as dust activity indicator during four months (April to July) was >20 which is close to the dust activities of primary global dust sources in the Middle East region (Arabia (southern Oman/Saudi border) with AAI values >21 and

average annual rainfall <100 mm (Goudie and Middleton, 2006; Shepherd et al., 2016). There is much less dust activity in the study area (especially in January) during the cold period.

In addition to AAI data, wind and visibility data from ground-level measurements were also screened using the criterion 10-m wind speed >20 kn, and all the potential events have been identified. The wind speeds are generally high during the warm period, especially in May, June, and July. Finally, sand and dust storm & severe sand and dust storm occasions were verified by comparing the identified events with the matching daily AAI data. Table 1 summarizes the monthly frequencies of the storms for the study region. The total number of the sand and dust storms (severe sand and dust storms) were 79 (13) in total (61 (8) episodes during the warm period, and 18 (and 5) episodes during the cold period). The highest prevalence values were recorded monthly in June (22 sand and dust storms and three severe sand and dust storms), and yearly in 2013 (17 sand and dust storms) and 2018 (three severe sand and dust storms).

Apart from the surface wind speed, other parameters are also affecting the occurrence of sand and dust storms. For example, the topsoil layer wetness is an essential factor in sand and dust emission potential, and it can be characterized by a combination of topsoil layer wetness and surface skin temperature using satellite data. It is well associated with soil texture and aggregate stability, aggregates size distribution, and soil organic matter content; it increases the strength of inter-particle bonds by developing a sticky film between particles (Aimar et al., 2012; Broomandi et al., 2017a; Liu et al., 2012). The topsoil layer wetness has high variability both in temporal and spatial scales. The wind emission prevails by the real wetness of the first top -centimeters of soil layer (Aimar et al., 2012).

The topsoil layer wetness and surface skin temperature from OMI have been studied to evaluate the impact of the topsoil layer wetness on the dust generation mechanism. The daily averages of the surface skin temperature experienced a considerable increase during the

warm period, particularly in June, July, and August (with the highest value of 317.7 °K in July). The topsoil layer wetness had a notable reduction during the warm period, particularly from June to September (with the minimum value of 2 in September). The study on the changes in topsoil wetness and surface skin temperature showed that the minimum value of wetness and maximum value of surface skin temperature were not recorded in June, whereas the highest wind speeds were experienced in June, confirming the critical role of 10-m wind speed in generating sand and dust storms.

Table 1. Monthly prevalence of dust storms (10-m wind speed >20 knots (kn)) and severe dust storms (10-m wind speed >30 kn) in the study area between 2007-2018 ("number of severe sand and dust storms" (in bold)/"number of sand and dust storms."

	Jan	**Feb**	**Mar**	**Apr**	**May**	**Jun**	**Jul**	**Aug**	**Sep**	**Oct**	**Nov**	**Dec**
2007	---	---	---	---	---	1	1	---	---	---	---	---
2008	---	---	---	---	2	**1**/2	1	---	1	---	---	---
2009	---	---	---	---	---	---	---	2	---	---	---	---
2010	---	---	---	**1**/1	---	1	**1**/2	---	---	---	---	---
2011	---	---	1	2	3	**1**/1	---	1	---	---	1	---
2012	---	---	2	---	---	3	---	---	---	---	---	**1**/2
2013	---	---	---	2	2	8	1	---	---	1	2	1
2014	---	---	1	1	---	2	---	---	---	---	---	---
2015	---	**2**/2	---	1	---	1	3	---	---	---	---	---
2016	---	---	---	---	1	---	1	1	**1**/2	**1**/1	1	---
2017	---	---	---	---	**1**/2	1	---	---	---	---	1	---
2018	**1**/1	---	---	**1**/3	---	**1**/1	3	---	1	---	---	1

A regression analysis was applied to the retrieved data from satellite and ground-based measurements (Figures 2 & 3). The regression analysis between annual & seasonal AAI distribution and surface skin temperature indicated a strong positive correlation, whereas a strong negative correlation was present between topsoil layer wetness and annual & seasonal AAI distribution. In June 2013 (the year with the highest annual occurrence of sand

and dust storms), the number of sand and dust storms reached its highest value (22). Finally, a strong correlation was also present between annual & seasonal AAI distribution and 10-m wind speed. The regression results show a lower tendency for dust emission following an increase in topsoil layer wetness and decrease in 10-m wind speed and surface skin temperature. These results are in good agreement with the literature (Almazroui et al., 2012; Namdari et al., 2018; Shafiee et al., 2016a, 2016b; Singh and Oh, 2007). Previous studies indicated that any increase in ambient air temperature causes a reduction in relative humidity, leading to a decrease in threshold wind speed to initiate dust emissions. Since previous studies confirmed that rainfall and temperature are two meteorological parameters which indirectly change the threshold friction velocity and directly determine topsoil layer wetness, further investigation of multivariable regression analysis by applying more parameters (temperature, rainfall, relative humidity) is recommended.

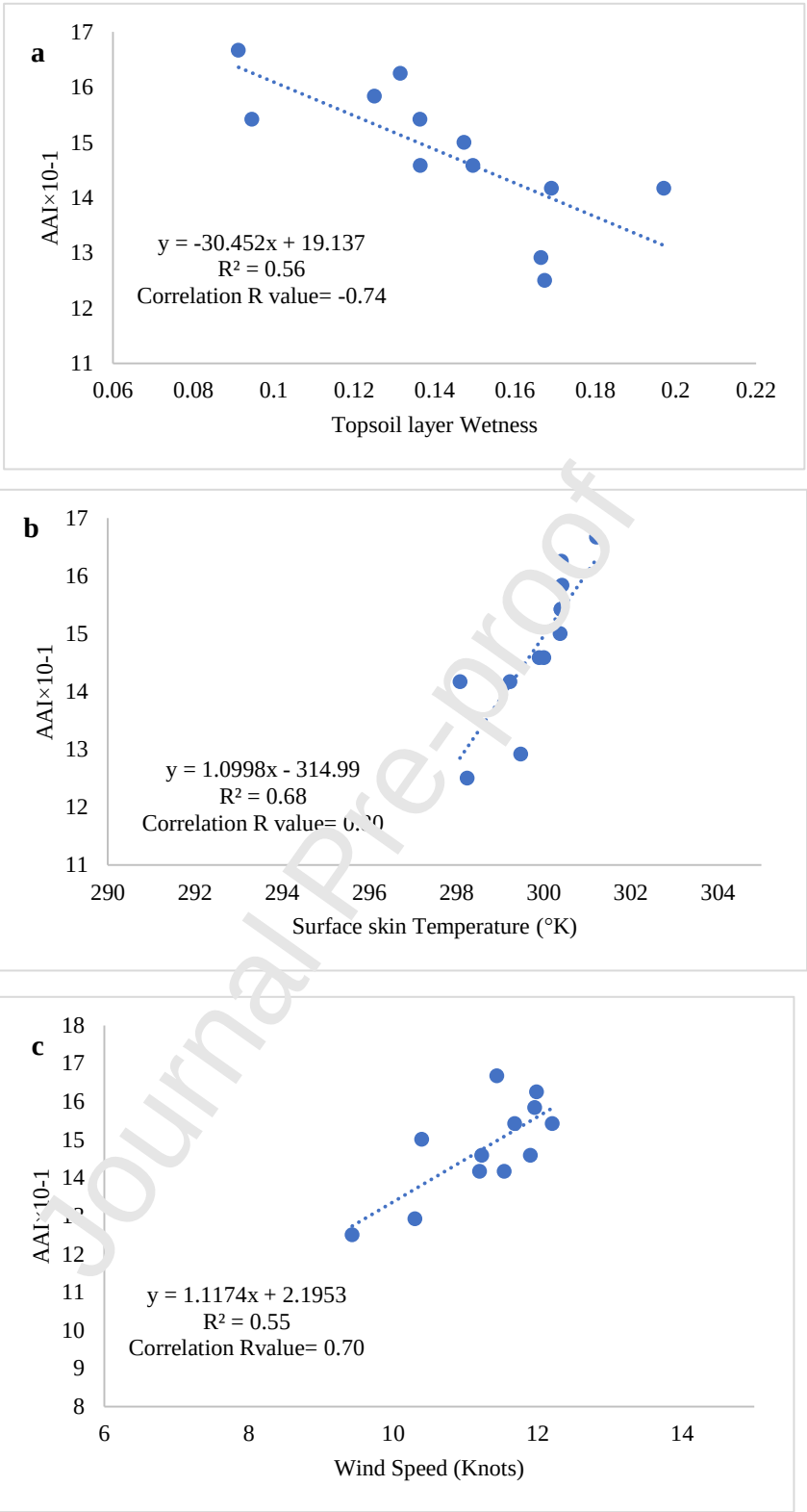

Figure 2. The regression analysis ($p < 0.001$) between annual AAI & topsoil layer wetness (a), surface skin temperature (b), and 10-m wind speed (c) between 2007 and 2018 in the study area, Shalamcheh, located in Khuzestan province, southwest Iran.

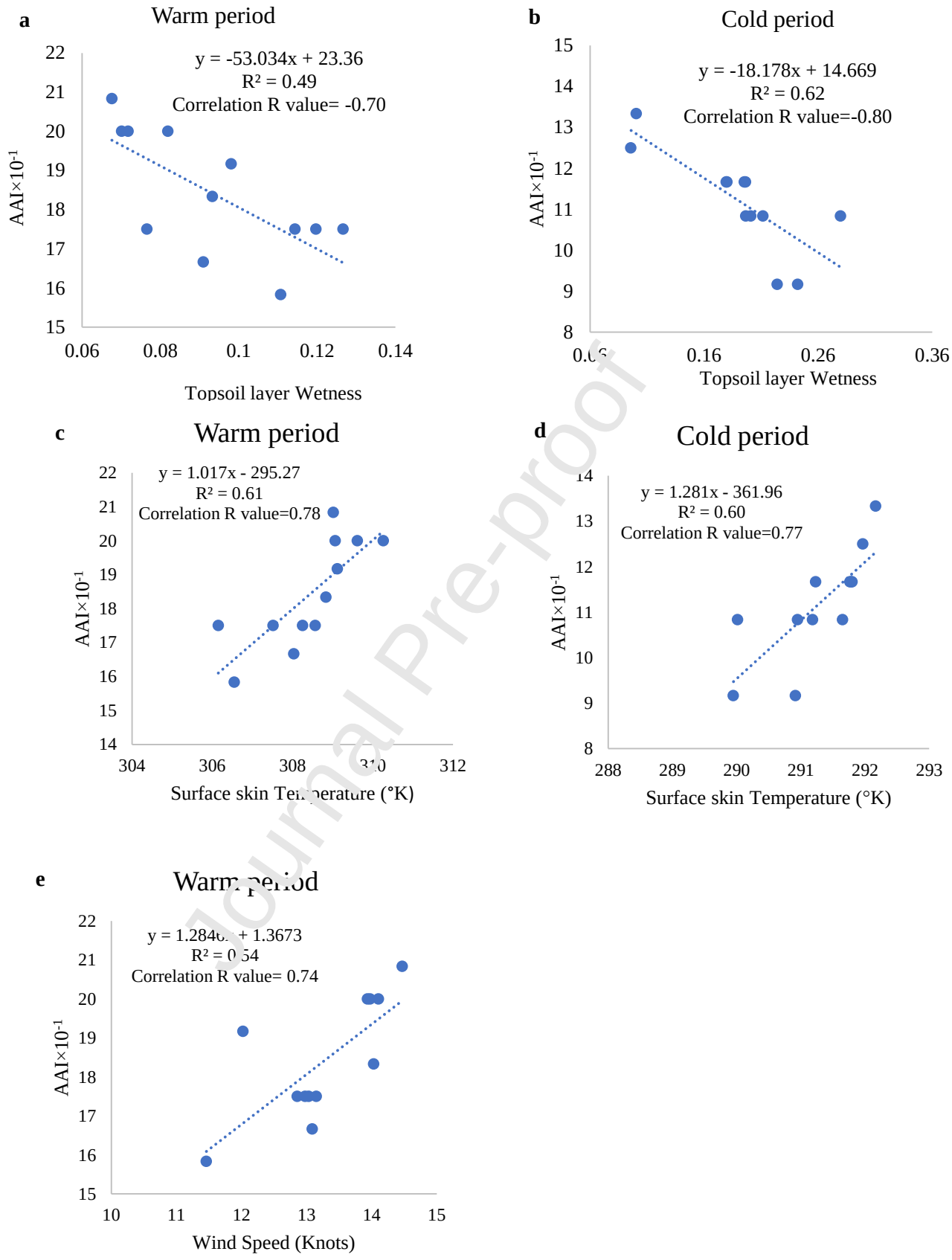

Figure 3. The regression analysis (p <0.001) between AAI & topsoil layer wetness (a & b), surface skin temperature (c & d), and 10-m wind speed (e & f) during warm and cold periods between 2007 and 2018 in area of study, Shalamcheh, located in Khuzestan province, southwest Iran.

3.2. Trajectory analysis in combination with AAI, topsoil layer wetness, and surface skin temperature data

The trajectory analysis was employed as a tool to assess the regional and long-range travel of the air parcels over the region for the identified events and episodes (numbers given in Table 1). Figures 4 & 5 present typical examples of the combined backward and forward trajectories of dust particles arriving and leaving the study area in combination with AAI, topsoil layer wetness, and surface skin temperature during the severe SDS events (10-m wind speed >30 kn) during the warm and cold periods. Backward trajectory analysis showed that air particles are loaded with dust particles from the central parts of Iraq before reaching Shalamcheh. However, the air parcels were further loaded while passing over the study area and deposited their load toward the Persian Gulf, Saudi Arabia, Yemen, and Arabian Sea

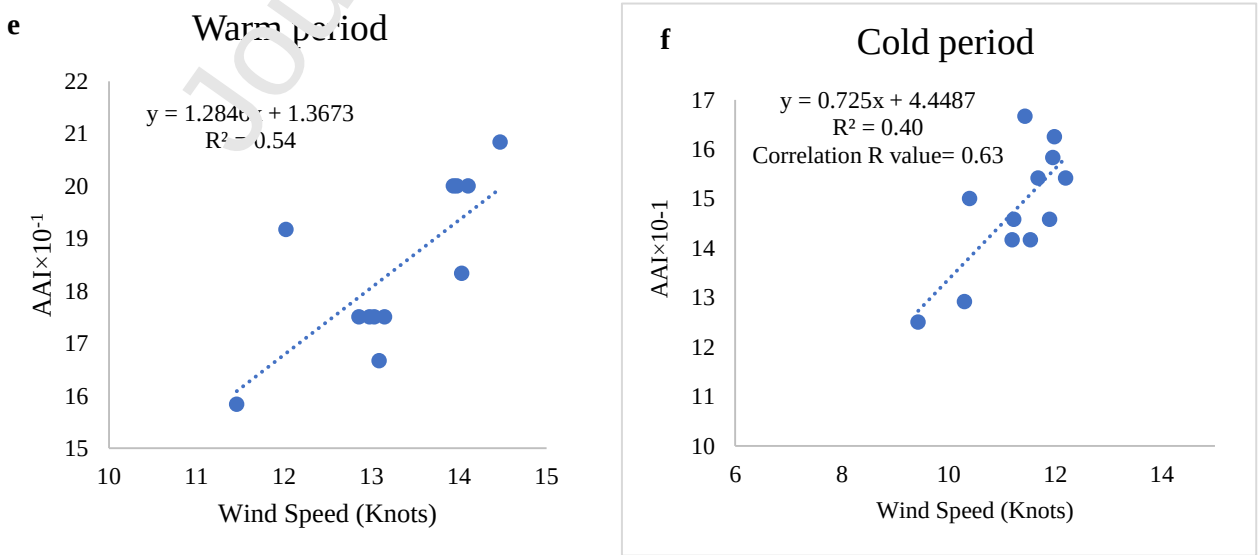

(e.g. Figure 4a on 07/06/2008). During the cold period, air particles were also loaded with dust particles passing some parts of the

Saudi Arabia border before reaching the study area (e.g., see Figure 5 on 02/10/2016). They continued their path toward central parts of Iran and then towards Central Asia after being further loaded over Shalamcheh area. During the warm and cold periods, the association between the dust activity (AAI) and topsoil characteristics (topsoil layer wetness and surface skin temperature) is statistically significant. Conversely, in some cases (e.g. Fig 4-b on 17/04/2010 in warm period & Fig 5-b on 21/12/2012 in cold period), despite strong wind and high surface skin temperature, the topsoil layer wetness was high and thus reduced the particle release. It is worth to mention that during both warm and cold seasons, we observed some anomalies in particle trajectories (e.g. Fig 4-b on 17/04/2010 & Fig S1-e on 22/04/2018 in warm period and Fig 5-a on 02/10/2016 & Fig S2-b on 20.02/2015 in cold period) and they did not follow the same discussed above-mentioned pattern as others did.

For the time frame studied in the present research, during the warm period, the topsoil layer wetness varied between 0.14 ± 0.05 (2011) and 0.06 ± 0.02 (2016) (Figures 4 & S1). Despite the higher averaged value of topsoil layer wetness in 2011, the averaged 10-m wind speed in 2011 (7.60 kn) was higher than that in 2016 (7.00 kn) resulting in a higher number of dust storms in 2011 compared to 2016. On the contrary, during the cold period, it ranged between 0.30 ± 0.14 (2015) and 0.15 ± 0.09 (2010) (Figures 5 & S2). However, the averaged 10-m wind speed in 2015 (5.00 kn) was higher than in 2010 (4.50 kn), leading to a higher number of dust storms in 2015 compared to 2010. According to Figures 4, 5, S1 and S2, relatively high and persistent AAI values are observed in the isolated origin areas such as north-eastern parts of Saudi Arabia, central parts of Iraq and Kuwait, and southwestern parts of Iran. The observed persistence of this specific area of intense dust activity suggests that locations in this area are specifically suitable for dust generation (Aimar et al., 2012; Broomandi et al., 2017b; Cao et al., 2015; Gholami et al., 2020; Shepherd et al., 2016).

The monthly average anomaly of topsoil layer wetness (0-10 cm underground) during 2007-2018 showed that there is a reduction in topsoil layer wetness in January, February, March, as well as in October (four of the six months of the cold season) which is strongly and positively correlated with monthly average rainfall anomalies during the same period (R^2 = 0.65, p <0.001). Previous research targeting the study area have pointed out that there are remarkable reductions in annual and seasonal (the cold and warm periods) anomaly values over 60 years (Broomandi et al., 2017a). Their regression analysis between yearly and seasonal meteorological parameters and the SDS occurrence also showed a positive correlation between SDS occurrence and wind speed (R^2 = 0.60, p <0.001) as well as SDS occurrence and temperature (R^2 = 0.60, p<0.001) whereas the SDS occurrence was negatively correlated with the rainfall (R^2 = -0.50, p <0.001) as well as with relative humidity (R^2 = -0.70, p <0.001) (Broomandi et al., 2017a). These reported high correlations between the soil properties and meteorological parameters indicate the increasing vulnerability of the study area with changing weather conditions in favor of wind erosion mechanism.

a) SDS event on 07/06/2008

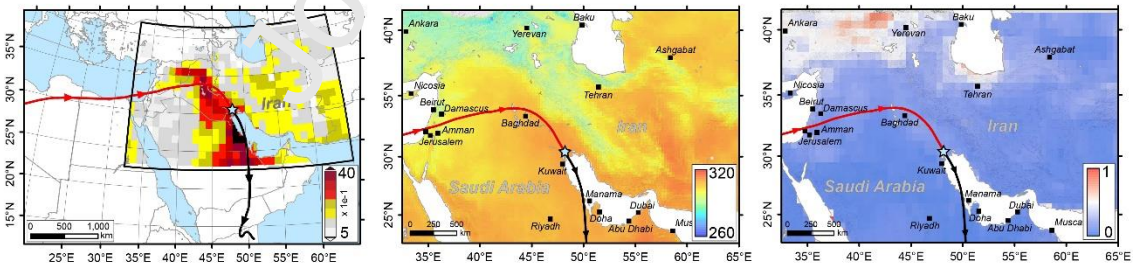

b) SDS event on 17/04/2010

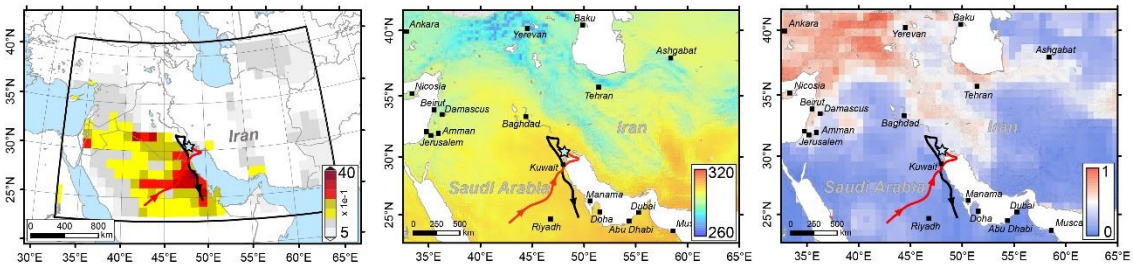

Figure 4. Warm period examples for backward-forward trajectories of dust particles arriving and leaving study area in combination with AAI, surface skin temperature (°K), and topsoil layer wetness (unitless) during a severe SDS event on (a) 07/06/2008, and (b) 17/04/2010

a) SDS event on 02/10/2016

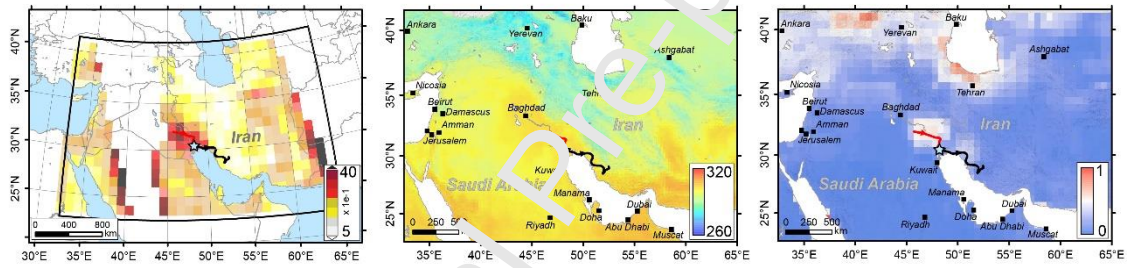

b) SDS event on 21/12/2012

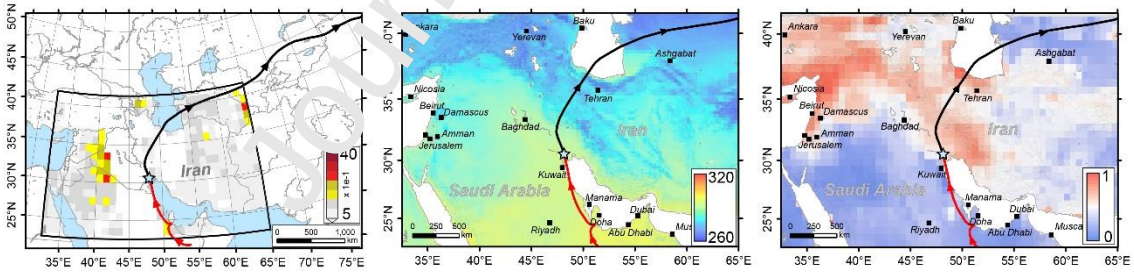

Figure 5. Cold period examples for backward-forward trajectories of dust particles arriving and leaving the study area in combination with AAI, surface skin temperature (°K), and topsoil layer wetness (unitless) during severe SDS events on (a) 02/10/2016, and (b) 21/12/2012.

3.3. Frequently impacted zones

The forward trajectories have been started at mid- atmospheric boundary layer (ABL) in order to capture its behavior under the ABL since the air-mass altitude in the dust lifecycle has vital roles within the ABL (Cavazos-Guerra and Todd, 2012; Meloni et al., 2008; Rashki et al., 2015). It interacts with the atmospheric dynamics by influencing the heating process under ABL and the dust deposition processes at ground level (Gautam et al., 2013; Kaskaoutis et al., 2012; Rashki et al., 2015). Generally, the air-mass forward pathways were similar in the cold and warm periods. The most significant difference was the observed higher numbers of events during the warm period, e.g., 22 sand and dust storms (three severe sand and dust storms) have been observed in June, and 12 sand and dust storms (one severe sand and dust storm) have been observed in July. The warm season trajectories also reached longer destinations along with broader spatial coverage, especially in July.

Fig. 6 and 7 present 72-hour air-mass forward trajectory frequencies, were originating from Shalamcheh during the sand and dust storm days of the warm and cold periods from 2007 to 2018. They show three frequency contours as the impact zones: (1) the maximum impact zone with 100% frequency (in both warm and cold periods), (2) the medium impact zone with >10% frequency (cold period) & >1% (warm period), and (3) the minimum impact zone with >1% frequency (cold period) & > 0.1% frequency (warm period) .

During the warm period, the dust-loaded air masses moved northwards, reaching Iraq, Turkey, Azerbaijan, Armenia, Georgia, Russia, and then turning toward northeastwards and affecting Afghanistan, Turkmenistan, Uzbekistan, Kazakhstan, Kyrgyzstan, Mongolia, and China. The areas within the impact zone furthermore included Jordan, Israel, Lebanon, and Syria. Air masses during these episodic events also moved to south and west, reaching Saudi Arabia, Emirates, Bahrain, Qatar, Yemen, Oman, Egypt, Eritrea, Sudan, Somalia, and Ethiopia. These systems also shifted southeastwards, affecting Pakistan and India (Figure 6). Kuwait was highly vulnerable to dust-loaded air systems and was located within the

maximum impact zone. Saudi Arabia, Iraq, Bahrain, Qatar, Emirates, Yemen, Oman, Syria, Jordan, Turkey, Azerbaijan, Armenia, and Turkmenistan were in the medium-impact zone. Finally, the dust-loaded air systems did hit not only the terrestrial environment but also the marine environment such as the Persian Gulf (frequency of 100%); Caspian Sea, Arabian Sea, Red Sea, Gulf of Aden (frequency >1%); and, the Black Sea (by frequency >0.1%) being frequent receptors during the warm periods in 2007-2018.

During the cold periods, the episodic air masses dispersed northwards and then turned toward northeastwards, affecting Iraq, Turkey, Syria, Azerbaijan, Armenia, Georgia, Russia, Afghanistan, Turkmenistan, Kazakhstan, and Uzbekistan (Figure 7). They also moved southwards, reaching Saudi Arabia, Bahrain, Qatar, Emirates, Yemen, and Oman. Kuwait was again highly vulnerable to episodic dust incursions and was located in the maximum impact zone. Saudi Arabia, Iraq, Bahrain, Qatar, Emirates, Yemen, and Oman were in the medium impact zone. Finally, the marine environment of the Persian Gulf (by frequency of 100%); Arabian Sea (by frequency >10%); Red Sea, Aral Sea, and Caspian Sea (by frequency >1%) have been affected by the events (Figure 7).

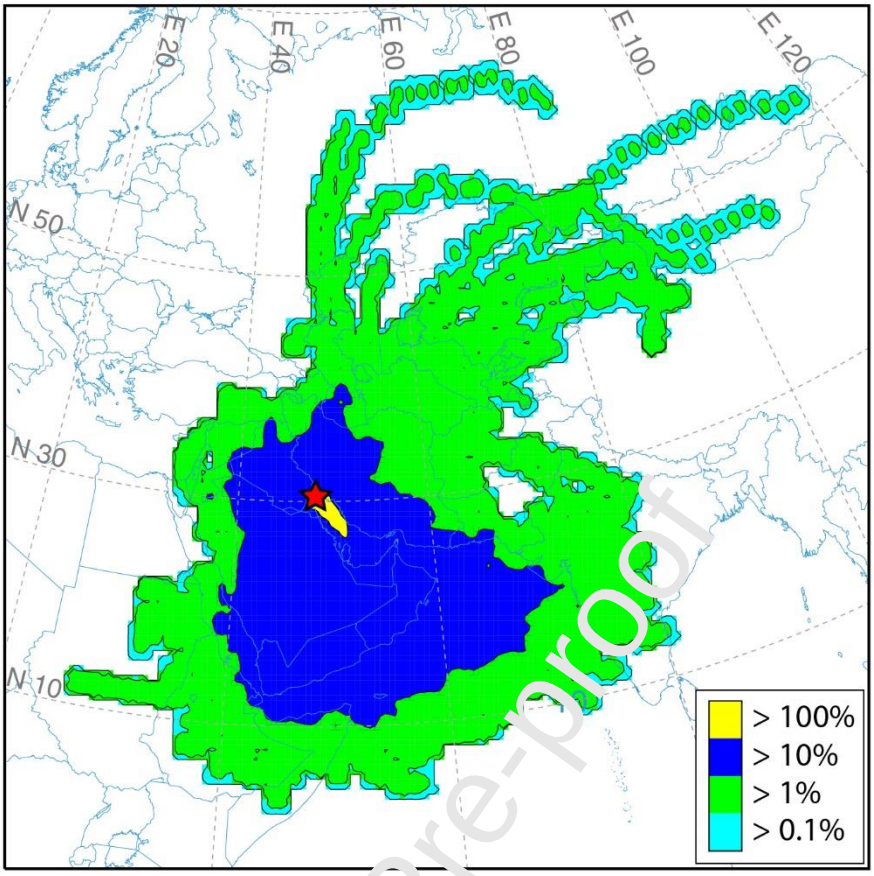

Figure 6. Forward trajectory frequency map for Shalamcheh (30°45’ N and 48° 15’E) using HYSPLIT-4 during the warm periods of the years between 2007 and 2018.

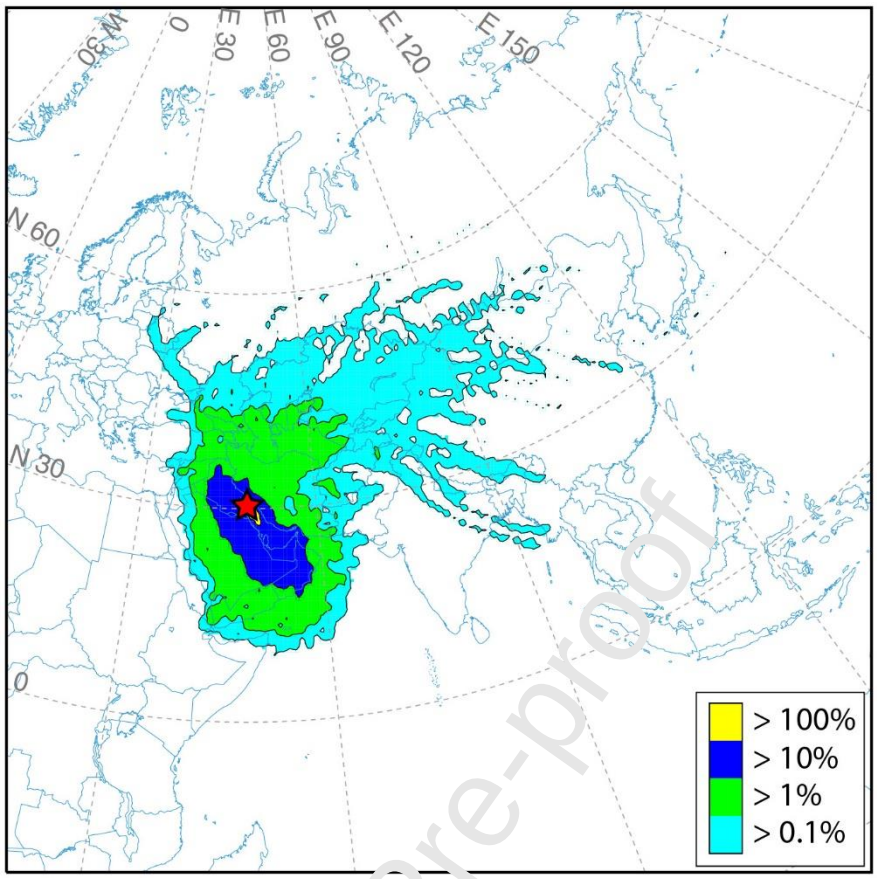

Figure 7. Forward trajectory frequency map for Shalamcheh (30°45’ N and 48° 15’E) using HYSPLIT-4 during the cold periods of the years between 2007 and 2018.

3.4. Regional transport pathways

Although the frequency maps are quite informative tools to assess the potential impacts zones, they do not provide a clear idea of the main transport pathways. Therefore, the HYSPLIT-4 clustering algorithm was used to identify the main routes of the identified episodes. This method clusters all the provided trajectories utilizing the change in the total spatial variance (TSV) parameter to determine the optimum number of clusters (Lu et al., 2018), and it has been used for the sand and dust storm events of the warm and cold periods during 2007–2018. The trajectory cluster groups, along with their frequencies for the warm and cold periods, are presented in Figure 8. During the warm period, the most frequent

receptors of the air masses carrying dust particles were Saudi Arabia, Iraq, Yemen, Oman, Kyrgyzstan, and Emirates (12%, 12%, 20%, 21%, and 2%, respectively). In the cold period, the most frequent receptor of the air masses carrying dust particles was Iraq (17%). In this time frame, local areas (Iran) also received dust particles (8%). Besides the terrestrial receptors, some marine environments were other main hosts for the air masses carrying dust particles originated or enriched from Shalamcheh: During the warm period, the Persian Gulf and Arabian sea were affected (12% and 20%, respectively). During the cold period, the Persian Gulf was the most frequent marine receptor of air masses (74%).

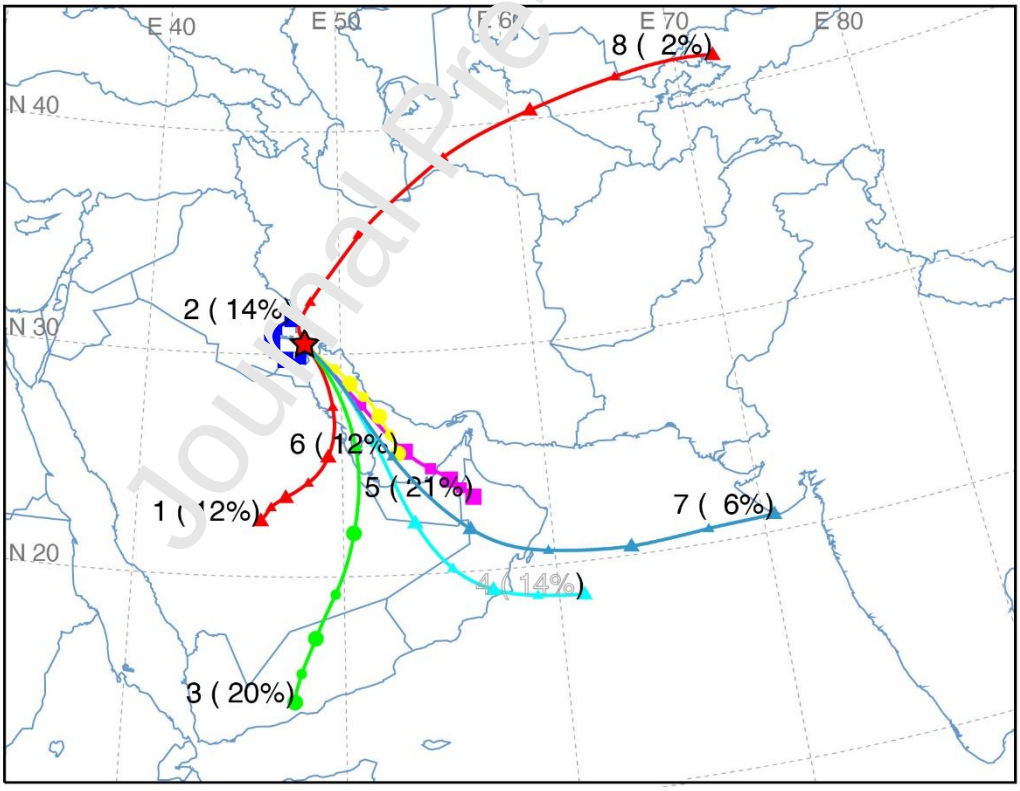

a) Trajectory cluster groups for warm period

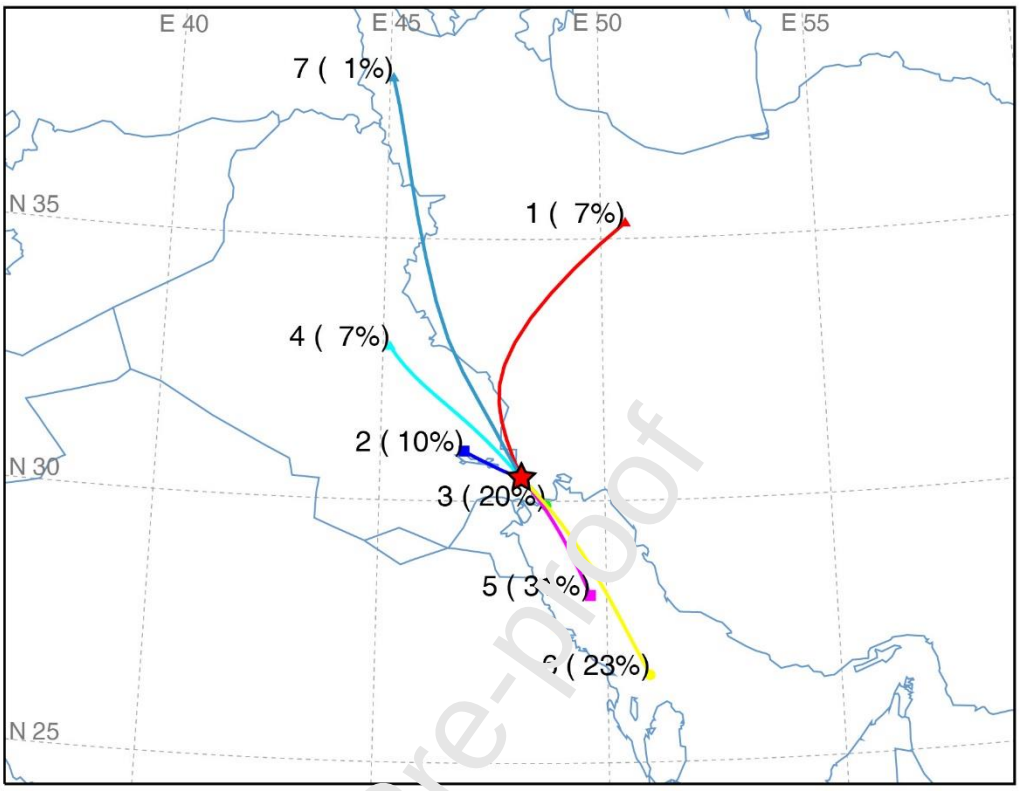

b) Trajectory cluster groups for cold period

Figure 8. Trajectory cluster groups with their frequencies for (a) warm and (b) cold periods between 2007 and 2018.

3.5. Dust deposition and potential impacts

It should be stated that the following discussion has been constructed based on the information from the literature and its relation to our findings thus are hypothetical. The results from the present study do not provide direct evidence on the environmental and health impacts on receptors since this study does not include any analysis in the receptor points and areas.

3.5.1. Mineral content

The long-range transport of windblown dust occurs with high temporal and spatial variability influenced by wet and dry deposition processes (Mahowald et al., 2017; Zhang et al., 2018; Zheng et al., 2016) and this could be experienced across continents and oceans, causing concerns in both terrestrial and marine ecosystems (Kok et al., 2017; Zhang et al., 2018) with levels exceeding 100 $g.m^{-2}$ deposition per year. Mineral dust particles contain macronutrients (such as silica and phosphate) and micronutrients (such as zinc and iron), which can enrich both terrestrial and marine ecosystems (Kohfeld and Tegen, 2007). For example, in marine environments, the long-range transport and subsequent deposition of dust aerosols can stimulate the growth of certain aquatic organisms due to the influx of nutrients as well as sequestrate carbon in the deep sea (Molloy and Mihaltcheva, 2013). Besides, dust particles by carrying the carbonates, are important sources of carbon for the alkaline carbon pool, capable of buffering the acidity of atmosphere and increasing the alkalinity of seawater, hence influencing large-scale environmental and climatic changes. As a result, while sand and dust storms (SDS) events can impact the atmosphere, they can reduce the acid deposition from the atmosphere and help the mitigation of global warming (Wang et al., 2017).

In the present study, the Persian Gulf could be the primary chronically affected marine ecosystem by the dust aerosol originated from Shalamcheh. The Persian Gulf (relatively shallow with a mean depth of 35 m) is located between Iran and the Arabian Peninsula. It is a semi-enclosed body of water that is only connected to the open waters through Hormuz Strait (Freije, 2015). It includes a variety of relatively sensitive ecosystems that are associated with an environment that is naturally under high stress and with poor flushing characteristics, very high evaporation rates, UV exposure, salinity, and elevated temperatures. Thus, contaminants are subject to a slower dispersion, limited dilution, and thus remain in the system for more extended times (de Mora et al., 2004; Freije, 2015). The seafood from the Persian Gulf (including fish and shrimp) is valuable and is subject to both

local consumption and export. As a result, it is essential to maintain good marine environmental quality for environmental, social, and economic reasons (Sheppard et al., 2010). Moreover, maintaining seawater quality is vital since many of the Gulf countries depend on the desalinated gulf water as a source of potable water for both domestic and industrial uses (Freije, 2015).

The soils of Shalamcheh are mainly constituted of SiO_2 with a mean value of 29.2%, and the total Fe content (as Fe_2O_3) of soil samples is 4.19% (ferric iron). SiO_2 and Fe_2O_3 content of dust particles was 31.9% and 2.13%, respectively, over Khoramshahr city (the nearest local terrestrial receptor) (Broomandi et al., 2017a). The ferric form of Fe that is dominant in aerobic environments is less soluble and occurs primarily as insoluble precipitates. Therefore, to obtain ferric iron, many aerobic microorganisms need to produce chelating iron-binding proteins capable of exchanging soluble Fe soluble and transporting it into the cell. In marine environments, by conducting an Fe fertilization study, researchers witnessed an increase in phytoplankton growth by the rate of two to three times background values. They have also discussed the influence of aeolian Fe on marine primary productivity rates in the iron-limited waters of the North Pacific (Griffin and Kellogg, 2004).

In contrast to supplying Fe by dust deposition in marine environment, it might be crucial to consider the role of the deposited dust in the scavenging of dissolved iron. In regions with high Fe concentrations, dust deposition acts as a net sink of dissolved Fe if the scavenging removal would exceed the Fe input by dust deposition (Ye et al., 2011; Ye and Völker, 2017). Generally, dust depositions act as an Fe input comparing to lithogenic scavenging in most parts of the Atlantic, but dust deposition could act as a net sink of dissolved Fe in some areas in the western part of the subtropical North Atlantic. Interestingly, a decrease of about 3% is witnessed in the global net primary production and export production, especially in the areas with high-nutrient low-chlorophyll like equatorial Pacific

and the Southern Ocean. It shows that lithogenic scavenging can globally impact marine productivity, even if the amplitude of the total change is small (Ye and Völker, 2017).

Also, previous studies suggested a possible association among dust storms and Fe and P enrichments in oceans (Tagliabue et al., 2017). Atmospheric dust fallout could result in the deposition of more than 60 Tg Fe and 1 Tg P into the world oceans (Mahowald et al., 2017). Also, Fe in dust aerosols may couple with anthropogenic S in the atmosphere and oceans, enhancing solubility and subsequent availability to aquatic organisms (Zhuang et al., 1992).

Besides the Persian Gulf as the probable primary chronically affected marine ecosystem, Kuwait could be the main terrestrial ecosystem chronically affected by the dust aerosol originated from Shalamcheh. Since dust particle's composition can vary from place to place due to the various origins, seasons, and weather conditions, it is critical to have a better understanding of PM sources and their characteristics to propose appropriate tailored mitigation strategies. Previous studies demonstrated that Kuwait city with a high rate of dust deposition (0.6 $Kg.m^{-2}.year^{-1}$) is ranked the first out of 56 dust deposition rates observed worldwide (Al-Awadhi and Alshuaibi, 2013; Al-Dousari and Al-Awadhi, 2012; Al-ThaniHanadi, 2018). Using satellite data and meteorological data, settled dust in Kuwait with lower clay minerals and higher carbonates comparing to the dust in the Sahara Desert were mainly originated the drained marshes in southern Iraq and Iran, the Mesopotamian Flood Plain, the north-eastern desert of Saudi Arabia, and the western desert of Iraq (Al-Dousari and Al-Awadhi, 2012; Al-ThaniHanadi, 2018). The deposited dust samples were mainly consisting of quartz (44%), followed by a high amount of calcite (Al-Dousari and Al-Awadhi, 2012; Al-ThaniHanadi, 2018).

3.5.2. War remains

Potentially toxic elements (PTEs) are ubiquitously used in and/or discharged by numerous domestic and industrial sectors. They are mostly found in relatively low concentrations in soils, rocks, and in natural atmospheric and aquatic environments.

Anthropogenic activities can dramatically disrupt and influence their distribution in natural systems. The Persian Gulf has previously faced substantial environmental stress over three decades via contamination by petroleum hydrocarbons and PTEs: during the Iraq–Iran War between 1980 and 1988, and during the first and second Gulf Wars in 1991 and 2003. Therefore, it can be hypothesized that one of the primary anthropogenic sources of contaminants in the area is war remains.

The EF values for selected trace and major elements from soil samples taken from Shalamcheh showed that Br, Cl, Mo, S, Zn, and Hg are of anthropogenic origin in the study area(Broomandi et al., 2017a). The war remains from Iraq-Iran could be one of the critical anthropogenic sources of trace elements in this area. Furthermore, high values of Cl and S encountered in the local soils could be attributed to chemical warfare (the use of chemical agents such as mustard gas) in the Iraq- Iran war during the period 1980-1988 (Broomandi et al., 2017a; Ghanbarizadeh and Nejad, 2012). It has been shown that the presence of Pb, Cu, Hg, Br, Mo, and Zn in contaminated soils could be linked to intense war activities (Wallace, 2018). The enriched Hg in the location may also be linked to war activities (Broomandi et al., 2017a).

Previous studies estimated possible dry deposited amounts of certain elements (Br, Mo, S, Zn, Ni, Cr, Co, and Hg) over Ahvaz city as a local receptor of dust particles originated from Shalamcheh in 2010 (Broomandi et al., 2018). Br, Mo, S, Zn and Hg identified as potential soil contaminants in the study area also had high EF values in the fallout dust particles over Ahvaz city in 2010. Their presence in Ahvaz airborne dust has been attributed to possible non-crustal sources such as fossil fuel combustion, traffic emissions, gas and

drilling activities, upstream petroleum industry (in Khuzestan or neighbouring dust origin areas in Iraq and Saudi Arabia), and remains of the Iraq-Iran war (Broomandi et al., 2018).

Therefore, the Persian Gulf, as the probable primary chronically affected marine ecosystem, by the dust aerosol originated from the war impacted area of Shalamcheh can be harmful to marine organisms and their ecosystem. According to the provided data by Paytan et al. (2009), frequent sand and dust storm events act as an essential source of both marine nutrient and terrestrial contaminants to the marine environments. The high levels of heavy metals (such as Cu and Pb), the toxic organic matter (such as polyaromatic hydrocarbon), and the interaction among dust particles and the contaminants during the transport can bring harm to the marine organisms and ecosystems. Studies showed that the presence of toxic substances carried by dust particles could increase the coral mortality rate in the Caribbean Sea (Paytan et al., 2009; Wang et al., 2017).

4. Conclusions, Implications, and Limitations

The present research assessed the seasonal formation (cold and warm periods) and the prevalence of sand and dust storms (SDSs) originated from a potential SDS area (Shalamcheh region southwest Iran) during 2007-2018; and, assessed the long-range transport pathways along with potential impact zones. The persistence of intense dust activity (especially during the warm period) suggests that the study area is a potential dust generation source at a global scale.

It is suggested that a decrease in topsoil layer wetness during the warm period resulted in increasing concentrations of absorbing aerosol in the atmospheric column. The saltation, resuspension, and/or creeping of sand particles start with certain controlling weather conditions (e.g., wind speed and topsoil layer wetness), which are required to be at specific

thresholds based on the sand particle characteristics (e.g., size, shape, and density) of the topsoil. Following the resuspension process, they can be transported over long distances.

Overall, the results indicated that the study area acts as an SDS source in the region. Based on the Total Zone Mapping Spectrometer data, the recorded severe and arid conditions in the area showed that it is a vulnerable dust source with a persistent average annual rainfall of under 100 mm (Goudie and Middleton, 2006) that makes the area a potential location prone to desertification. The susceptibility of the study area to turn into a permanent dust source with desertification has also been mentioned in other studies (Broomandi et al., 2017a; Cao et al., 2015; Heidarian et al., 2018). Dust-storm pathways from Sahara towards the tropical Atlantic, the Mediterranean, and the Middle East have been well documented (Awad and Mashat, 2013; Liu et al., 2012). In Iran, those originating from the Sistan basin were also examined (Rashki et al., 2015), but those originating from Shalamcheh have yet to be studied. To the best of our knowledge, the current study is the first that examines the dust-transport pathways and the regional areas affected by the Shalamcheh sand and dust storms in full scale.

The trajectory modelling has identified long-distance receptor areas (impact zones), indicating that numerous countries, as well as marine zones, receive dust from the area (Kuwait and the Persian Gulf under particular high impact), which might significantly affect nutrient as well as potentially toxic element (PTE) profile of the environment. Regarding the high wind vulnerability of the study area, which is also a war-impacted region with a potential presence of PTEs and other toxic substances, contaminated dust particles may be transported over not only the surrounding region but also long distances, including agricultural land and marine environment. Previous studies on the Persian Gulf have already reported elevated levels of 11 trace PTEs (including Zn, As, Cr, Cu, Pb, Ni, Cd, and Hg), mainly in marine and coastal areas (Fowler et al., 2007; Freije, 2015; Juma and Al-Madany,

2008; Naser, 2009). As the study area is now identified as a source of SDS and it is at the same time a war-impacted area, potentially contaminated, it is recommended to perform site characterization studies taking major war-impacted zones into account. It is highly recommended to take effective functional stabilizing methods to control the wind erosion on susceptible regions of the study area.

One of the main limitations of the present study is the lack of on-site meteorological and air quality stations, which made the study rely on the closest available stations (Abadan and Khoramshahr meteorological stations, Khorramshahr air quality station). Also, for the time frame studied, the availability of PM_{10} data, measured at Khorramshahr air quality station (the nearest station to the area of interest), was below 50% which prevented our team from performing statistical analyses to investigate the relationship between measured ground-based PM_{10} and retrieved AAI data. Finally, topsoil layer wetness and surface skin temperature values have not been measured in any of the ground stations; thus, it was not possible to investigate the relationship between measured ground-based data and satellite-retrieved data.

Acknowledgement

This project has received funding from the European Union's Horizon 2020 research and innovation program Marie Skłodowska-Curie Actions Research and Innovation Staff Exchange (RISE) under grant agreement No. 778360 and NU project (Nazarbayev Research Fund SOE2017004).

The authors would like to thank all reviewers for their time and appreciate their valuable comments which have significantly contributed to the improvement of the quality of this manuscript.

Conflict of interest

The authors declare that they have no conflict of interest.

References:

Ahvaz IRIMO, 2016. Iranian Meteorological Office Data Processing Center. Ahvaz: Islamic Republic of Iran Meteorological Office.

Aimar, S.B., Mendez, M.J., Funk, R., Buschiazzo, D.E., 2012. Soil properties related to potential particulate matter emissions (PM10) of sandy soils. Aeolian Res. 3, 437–443. https://doi.org/10.1016/J.AEOLIA.2010.12.001

Al-Awadhi, J., Alshuaibi, A., 2013. Dust fallout in Kuwait city: Deposition and characterization. Sci. Total Environ. 461-462C, 139–148. https://doi.org/10.1016/j.scitotenv.2013.03.052

Al-Dousari, A., Al-Awadhi, J., 2012. Dust fallout in northern Kuwait, major sources and characteristics. Kuwait J. Sci. Eng. 39, 171–187.

Al-ThaniHanadi, M.K.R.I.J.., 2018. Investigations on Deposited Dust Fallout in Urban Doha: Characterization, Source Apportionment and Mitigation. Environ. Ecol. Res. 6.5, 493–506. https://doi.org/10.13189/eer.2018.060510

Almazroui, M., Islam, M., Hussain, A., Jones, P., Rahman, M., 2012. Recent climate change in the Arabian Peninsula: Annual rainfall and temperature analysis of Saudi Arabia for 1978–2009. Int. J. Climatol. 32, 953–966. https://doi.org/10.1002/joc.3446

Ashrafi, K., Shafiepour-Motlagh, M., Aslemand, A., Ghader, S., 2014. Dust storm simulation over Iran using HYSPLIT. J. Environ. Heal. Sci. Eng. 12, 9. https://doi.org/10.1186/2052-336X-12-9

Awad, A., Mashat, A., 2013. Synoptic features associated with dust transition processes from North Africa to Asia. Arab. J. Geosci. 7. https://doi.org/10.1007/s12517-013-0923-4

Broomandi, P., Dabir, B., Bonakdarpour, B., Rashidi, Y., 2017a. Identification of dust storm origin in South -West of Iran. J. Environ. Heal. Sci. Eng. 15, 16.

https://doi.org/10.1186/s40201-017-0280-4

Broomandi, P., Dabir, B., Bonakdarpour, B., Rashidi, Y., 2017b. Identification of the sources of dust storms in the City of Ahvaz by HYSPLIT. Pollution 3, 341–348. https://doi.org/10.7508/pj.2017.02. 015

Broomandi, P., Dabir, B., Bonakdarpour, B., Rashidi, Y., Akherati, A., 2018. Simulation of mineral dust aerosols in southwestern iran through numerical prediction models. Environ. Prog. Sustain. Energy 37, 1380–1393. https://doi.org/10.1002/ep.12805

Cao, H., Amiraslani, F., Liu, J., Zhou, N., 2015. Identification of dust storm source areas in West Asia using multiple environmental datasets. Sci. Total Environ. 502, 224–235. https://doi.org/10.1016/J.SCITOTENV.2014.09.025

Cavazos-Guerra, C., Todd, M.C., 2012. Model Simulations of Complex Dust Emissions over the Sahara during the West African Monsoon Onset. Adv. Meteorol. 2012, 351731. https://doi.org/10.1155/2012/351731

de Mora, S., Fowler, S.W., Wyse, E., Azemard, S., 2004. Distribution of heavy metals in marine bivalves, fish and coastal sediments in the Gulf and Gulf of Oman. Mar. Pollut. Bull. 49, 410–424. https://doi.org/10.1016/J.MARPOLBUL.2004.02.029

de Villiers, M., van Heerden, J., 2011. Nakhi dust storm over the United Arab Emirates. Weather 66, 79–81. https://doi.org/10.1002/wea.727

Dipu, S., Prabha, T. V., Panditkurai, G., Dudhia, J., Pfister, G., Rajesh, K., Goswami, B.N., 2013. Impact of elevated aerosol layer on the cloud macrophysical properties prior to monsoon onset. Atmos. Environ. 70, 454–467. https://doi.org/10.1016/J.ATMOSENV.2012.12.036

Draxler, R., Hess, G., 1997. Description of the HYSPLIT_4 modelling system. NOAA Tech. Mem. ERL ARL-224.

Dunion, J., Velden, C., 2002. The Impact of the Saharan Air Layer on Atlantic Tropical Cyclone Activity. AGU Spring Meet. Abstr. 1, 08. https://doi.org/10.1175/BAMS-85-3-353

Ekhtesasi, M.R., Gohari, Z., 2012. Determining Area Affected by Dust Storms in Different WindSpeeds, Using Satellite Images. Desert 17, 193–202. https://doi.org/10.22059/jdesert.2013.32035

Esmaili, O., Tajrishy, M., Daneshkar Arasteh, P., 2006. Results of the 50 year ground-based measurements in comparison with satellite remote sensing of two prominent dust emission sources located in Iran. Proc. SPIE - Int. Soc. Opt. Eng. 6362. https://doi.org/10.1117/12.692989

Fowler, S., Villeneuve, J.-P., Wyse, E., Jupp, B., De Mora, S., 2007. Temporal survey of petroleum hydrocarbons, organochlorinated compounds and heavy metals in benthic marine organisms from Dhofar, southern Oman. Baseline 1. Mar. Pollut. Bull. 54, 357–367. https://doi.org/10.1016/j.marpolbul.2006.11.027

Freije, A.M., 2015. Heavy metal, trace element and petroleum hydrocarbon pollution in the Arabian Gulf: Review. J. Assoc. Arab Univ. Basic Appl. Sci. 17, 90–100. https://doi.org/10.1016/J.JAUBAS.2014.02.001

Gautam, R., Hsu, N.C., Lau, W.K.-M., Yasunari, T.J., 2013. Satellite observations of desert dust-induced Himalayan snow darkening. Geophys. Res. Lett. 40, 988–993. https://doi.org/10.1002/grl.50226

Ghanbarizadeh, L., Nejad, T.S., 2012. Change patterns of agronomy and agricultural lands by war. Life Sci. J. 9, 1454–1462.

Gholami, H., Rahimi, S., Fathabadi, A., Habibi, S., Collins, A., 2020. Mapping the spatial sources of atmospheric dust using GLUE and Monte Carlo simulation. Sci. Total Environ. 723. https://doi.org/10.1016/j.scitotenv.2020.138090

Ginoux, P., Prospero, J., Gill, T., Hsu, N., Zhao, M., 2012. Global-scale attribution of anthropogenic and natural dust sources and their emission rates based on MODIS Deep Blue aerosol products. Rev. Geophys. 50, 3005-. https://doi.org/10.1029/2012RG000388

Goudarzi, G., Alavi, N., Geravandi, S., Idani, E., Behrooz, H.R.A., Babaei, A.A., Alamdari, F.A., Dobaradaran, S., Farhadi, M., Mohammadi, M.J., 2018. Health risk assessment on human exposed to heavy metals in the ambient air PM10 in Ahvaz, southwest Iran. Int. J. Biometeorol. 62, 1075–1083. https://doi.org/10.1007/s00484-018-1510-x

Goudie, A., Middleton, N., 2006. Desert Dust in the Global System. Desert Dust Glob. Syst. 1–287. https://doi.org/10.1007/3-540-32355-4

Griffin, D., Kellogg, C., 2004. Dust Storms and Their Impact on Ocean and Human Health: Dust in Earth's Atmosphere. Ecohealth 1, 284–295. https://doi.org/10.1007/s10393-004-0120-8

Heidarian, P., Azhdari, A., Joudaki, M., Khatooni, J.D., Firoozjaei, S.F., 2018. Integrating Remote Sensing, GIS, and Sedimentology Techniques for Identifying Dust Storm Sources: A Case Study in Khuzestan, Iran. J. Indian Soc. Remote Sens. 46, 1113–1124. https://doi.org/10.1007/s12524-018-0774-2

Jickells, T.D., An, Z.S., Andersen, K.K., Baker, A.R., Bergametti, G., Brooks, N., Cao, J.J., Boyd, P.W., Duce, R.A., Hunter, K.A., Kawahata, H., Kubilay, N., laRoche, J., Liss, P.S., Mahowald, N., Prospero, J.M., Ridgwell, A.J., Tegen, I., Torres, R., 2005. Global Iron Connections Between Desert Dust, Ocean Biogeochemistry, and Climate. Science (80-.). 308, 67 LP – 71. https://doi.org/10.1126/science.1105959

Juma, H., Al-Madany, I., 2008. Concentration of Heavy Metals in the Territorial Sea Water of the Kingdom of Bahrain, Arabian Gulf. Arab Gulf J. Sci. Res. 26, 19–32.

Karimi, N., Moridnejad, A., Golian, S., J.M.V, S., Karimi, D., Javadi, S., 2012. Comparison of dust source identification techniques over land in the Middle East region using MODIS data. Can. J. Remote Sens. 38, 586–599. https://doi.org/10.5589/m12-048

Kaskaoutis, D.G., Nastos, P.T., Kosmopoulos, P.G., Kambezidis, H.D., 2012. Characterising the long-range transport mechanisms of different aerosol types over Athens, Greece during 2000–2005. Int. J. Climatol. 32, 1249–1270. https://doi.org/10.1002/joc.2357

Kessler, N., Armoza-Zvuloni, R., Wang, S., Basu, S., Weber, P., Stuart, R., Shaked, Y., 2019. Selective collection of iron-rich dust particles by natural Trichodesmium colonies. ISME J. 14. https://doi.org/10.1038/s41396-019-0505-x

Kohfeld, K.E., Tegen, I., 2007. Record of Mineral Aerosols and Their Role in the Earth System. Treatise on Geochemistry 1–26. https://doi.org/10.1016/B978-008043751-4/00236-4

Kok, J.F., Ridley, D.A., Zhou, Q., Miller, R.L., Zhao, C., Heald, C.L., Ward, D.S., Albani, S., Haustein, K., 2017. Smaller desert dust cooling effect estimated from analysis of dust size and abundance. Nat. Geosci. 10, 274–278. https://doi.org/10.1038/ngeo2912

Lemaitre, C., Flamant, C., Cuesta, J., Raut, J.-C., Chazette, P., Formenti, P., Pelon, J., 2010. Radiative heating rates profiles associated with a springtime case of Bodélé and Sudan dust transport over West Africa. Atmos. Chem. Phys. 10. https://doi.org/10.5194/acp-10-8131-2010

Liu, D., Wang, Y., Wang, Z., Zhou, J., 2012. The Three-Dimensional Structure of

Transatlantic African Dust Transport: A New Perspective from CALIPSO LIDAR Measurements. Adv. Meteorol. 2012, 850704. https://doi.org/10.1155/2012/850704

Lu, X., Mao, F., Pan, Z., Gong, W., Wei, W., Tian, L., Fang, S., 2018. Three-dimensional physical and optical characteristics of aerosols over central China from long-term CALIPSO and HYSPLIT data. Remote Sens. 10, 314. https://doi.org/10.3390/rs10020314

Maghrabi, A., Alharbi, B., Tapper, N., 2011. Impact of the March 2009 dust event in Saudi Arabia on aerosol optical properties, meteorological parameters, sky temperature and emissivity. Atmos. Environ. 45, 2164–2173. https://doi.org/10.1016/J.ATMOSENV.2011.01.071

Mahowald, N.M., Scanza, R., Brahney, J., Goodale, C.L., Hess, P.G., Moore, J.K., Neff, J., 2017. Aerosol Deposition Impacts on Land and Ocean Carbon Cycles. Curr. Clim. Chang. Reports 3, 16–31. https://doi.org/10.1007/s40641-017-0056-z

Martiny, N., Chiapello, I., 2013. Assessments for the impact of mineral dust on the meningitis incidence in West Africa. Atmos. Environ. 70, 245–253. https://doi.org/10.1016/J.ATMOSENV.2013.01.016

Meloni, D., di Sarra, A., Monteleone, F., Pace, G., Piacentino, S., Sferlazzo, D.M., 2008. Seasonal transport patterns of intense Saharan dust events at the Mediterranean island of Lampedusa. Atmos. Res. - ATMOS RES 88, 134–148. https://doi.org/10.1016/j.atmosres.2007.10.007

Merrifield, A., Schindeler, S., Jalaludin, B., Smith, W., 2013. Health effects of the September 2009 dust storm in Sydney, Australia: Did emergency department visits and hospital admissions increase? Environ. Health 12, 32. https://doi.org/10.1186/1476-069X-12-32

Miri, A., Ahmadi, H., Ghanbari, A., Moghaddamnia, A., 2007. Dust Storms Impacts on Air Pollution and Public Health under Hot and Dry Climate. Int. J. Energy Environ. 2(1).

Mohammadi, M., Geravandi, S., Vosoughi Niri, M., Salmanzadeh, S., Goudarzi, G., 2015. An Association between air quality and COPD in Ahvaz, Iran. Jundishapur J. Chronic Dis. Care 4. https://doi.org/10.5812/jjcdc.26621

Molloy, S.L., Mihaltcheva, S., 2013. Extreme Weather Events. Clim. Vulnerability 3–16. https://doi.org/10.1016/B978-0-12-384703-4.00103-9

Naimabadi, A., Ghadiri, A., Idani, E., Babaei, A.A., Alavi, N., Shirmardi, M., Khodadadi, A.,

Marzouni, M.B., Ankali, K.A., Rouhizadeh, A., Goudarzi, G., 2016. Chemical composition of PM10 and its in vitro toxicological impacts on lung cells during the Middle Eastern Dust (MED) storms in Ahvaz, Iran. Environ. Pollut. 211, 316–324. https://doi.org/10.1016/J.ENVPOL.2016.01.006

Namdari, S., Karimi, N., Sorooshian, A., Mohammadi, G., Sehatkashani, S., 2018. Impacts of climate and synoptic fluctuations on dust storm activity over the Middle East. Atmos. Environ. (1994). 173, 265–276. https://doi.org/10.1016/j.atmosenv.2017.11.016

Naser, H., 2009. Testing taxonomic resolution levels for detecting environmental impacts using macrobenthic assemblages in tropical waters. Environ. Monit. Assess. 170, 435–444. https://doi.org/10.1007/s10661-009-1244-7

Paytan, A., Mackey, K.R.M., Chen, Y., Lima, I.D., Doney, S.C., Mahowald, N., Labiosa, R., Post, A.F., 2009. Toxicity of atmospheric aerosols on marine phytoplankton. Proc. Natl. Acad. Sci. U. S. A. 106, 4601–4605. https://doi.org/10.1073/pnas.0811486106

Prasad, A., Yang, K.-H., El-Askary, H., Kafatos, M., 2009. Melting of Major Glaciers in the Western Himalayas: Evidence of Climatic Changes from Long Term MSU Derived Tropospheric Temperature Trend (1979-2008). Ann. Geophys. 27. https://doi.org/10.5194/angeo-27-1505-2009

Prijith, S.S., Rajeev, K., Thampi, B. V., Nair, S.K., Mohan, M., 2013. Multi-year observations of the spatial and vertical distribution of aerosols and the genesis of abnormal variations in aerosol loading over the Arabian Sea during Asian summer monsoon season. J. Atmos. Solar-Terrestrial Phys. 105–106, 142–151. https://doi.org/10.1016/J.JASTP.2013.09.009

Prospero, J.M., Ginoux, P., Torres, O., Nicholson, S.E., Gill, T.E., 2002. Environmental Characterization of Global Sources of Atmospheric Soil Dust Identified with the Nimbus 7 Total Ozone Mapping Spectrometer (TOMS) Absorbing Aerosal. Rev. Geophys. 40, 2-1-2–31. https://doi.org/10.1029/2000RG000095

Rashki, A., Kaskaoutis, D., Eriksson, P., Rautenbach, C., Flamant, C., Vishkaee, F., 2013. Spatio-temporal variability of dust aerosols over the Sistan region in Iran based on satellite observations. Nat. Hazards 71. https://doi.org/10.1007/s11069-013-0927-0

Rashki, A., Kaskaoutis, D.G., Francois, P., Kosmopoulos, P.G., Legrand, M., 2015. Dust-storm dynamics over Sistan region, Iran: Seasonality, transport characteristics and

affected areas. Aeolian Res. 16, 35–48. https://doi.org/10.1016/J.AEOLIA.2014.10.003

Salmabadi, H., Khalidy, R., Saeedi, M., 2020. Transport routes and potential source regions of the Middle Eastern dust over Ahvaz during 2005–2017. Atmos. Res. 241, 104947. https://doi.org/https://doi.org/10.1016/j.atmosres.2020.104947

Samadi, M., Darvishi Boloorani, A., Alavi Panah, S.K., Mohamadi, H., Najafi, M., 2014. Global dust Detection Index (GDDI); A new remotely sensed methodology for dust storms detection. J. Environ. Heal. Sci. Eng. 12, 20. https://doi.org/10.1186/2052-336X-12-20

Shafiee, M., Feghhi, S.A.H., Rahighi, J., 2016a. Numerical Analysis of the Beam Position Monitor Pickup for the Iranian Light Source Facility. Nucl. Instruments Methods Phys. Res. Sect. A Accel. Spectrometers, Detect. Assoc. Equip. 847. https://doi.org/10.1016/j.nima.2016.11.065

Shafiee, M., Feghhi, S.A.H., Rahighi, J., 2016b. Analysis of de-noising methods to improve the precision of the ILSF BPM electronic readout system. J. Instrum. 11, P12020–P12020. https://doi.org/10.1088/1748-0221/11/12/p12020

Shao, Y., Wyrwoll, K.-H., Chappell, A., Huang, J., Lin, Z., McTainsh, G.H., Mikami, M., Tanaka, T.Y., Wang, X., Yoon, S., 2011. Dust cycle: An emerging core theme in Earth system science. Aeolian Res. 2, 181–204. https://doi.org/10.1016/J.AEOLIA.2011.02.001

Shepherd, G., Terradellas, E., Baklanov, A., Kang, U., Sprigg, W., Nickovic, S., Darvishi Boloorani, A., Al-Dousari, A., Basart, S., Benedetti, A., Sealy, A., Tong, D., Zhang, X., Guillemot, J., Kebin, Z., Knippertz, P., Mohammed, A., Al-Dabbas, M., Cheng, L., Cha, J., 2016. Global Assessment of Sand and Dust Storms.

Sheppard, C., Al-Husiani, M., Al-Jamali, F., Al-Yamani, F., Baldwin, R., Bishop, J., Benzoni, F., Dutrieux, E., Dulvy, N.K., Durvasula, S.R. V., Jones, D.A., Loughland, R., Medio, D., Nithyanandan, M., Pilling, G.M., Polikarpov, I., Price, A.R.G., Purkis, S., Riegl, B., Saburova, M., Namin, K.S., Taylor, O., Wilson, S., Zainal, K., 2010. The Gulf: A young sea in decline. Mar. Pollut. Bull. 60, 13–38. https://doi.org/10.1016/J.MARPOLBUL.2009.10.017

Singh, G., Oh, J., 2007. Impact of Indian Ocean sea-surface temperature anomaly on Indian summer monsoon precipitation using a regional climate model. Int. J. Climatol. 27,

1455–1465. https://doi.org/10.1002/joc.1485

Singh, R., Prasad, A., Kayetha, V., Kafatos, M., 2008. Enhancement of oceanic parameters associated with dust storms using satellite data. J. Geophys. Res. 113. https://doi.org/10.1029/2008JC004815

Sorek-Hamer, M., Cohen, A., Levy, R., Ziv, B., Broday, D., 2013. Classification of dust days by satellite remotely sensed aerosol products. Int. J. Remote Sens. 34, 2672–2688. https://doi.org/10.1080/01431161.2012.748991

Tagliabue, A., Bowie, A.R., Boyd, P.W., Buck, K.N., Johnson, K.S., Saito, M.A., 2017. The integral role of iron in ocean biogeochemistry. Nature 543, 51–59. https://doi.org/10.1038/nature21058

Ueda, S., Miki, Y., Kato, H., Miura, K., Nakayama, H., Fukutani, H., Uematsu, M., 2020. Internal Structure of Asian Dust Particles over the Western North Pacific: Analyses Using Focused Ion Beam and Transmission Electron Microscopy. Atmosphere (Basel). 11, 78. https://doi.org/10.3390/atmos11010078

Wallace, J.S., 2018. Chemical Analysis of Firearms, Ammunition, and Gunshot Residue, 2nd editio. ed. CRC Press.

Wang, F., Zhao, X., Gerlein-Safdi, C., Mu, Y., Wang, D., Lu, Q., 2017. Global sources, emissions, transport and deposition of dust and sand and their effects on the climate and environment: a review. Front. Environ. Sci. Eng. 11, 13. https://doi.org/10.1007/s11783-017-0904-z

Ye, Y., Völker, C., 2017. On the Role of Dust-Deposited Lithogenic Particles for Iron Cycling in the Tropical and Subtropical Atlantic. Global Biogeochem. Cycles 31, 1543–1558. https://doi.org/10.1002/2017GB005663

Ye, Y., Wagener, T., Voelker, C., Guieu, C., Wolf-Gladrow, D., 2011. Dust deposition: Iron source or sink? A case study. Biogeosciences 8, 2107–2124. https://doi.org/10.5194/bg-8-2107-2011

Zhang, X.-X., Sharratt, B., Liu, L.-Y., Wang, Z.-F., Pan, X.-L., Lei, J.-Q., Wu, S.-X., Huang, S.-Y., Guo, Y.-H., Li, J., Tang, X., Yang, T., Tian, Y., Chen, X.-S., Hao, J.-Q., Zheng, H.-T., Yang, Y.-Y., Lyu, Y.-L., 2018. East Asian dust storm in May 2017: observations, modelling, and its influence on the Asia-Pacific region. Atmos. Chem. Phys. 18, 8353–8371. https://doi.org/10.5194/acp-18-8353-2018

Zheng, Y., Zhao, T., Che, H., Liu, Y., Han, Y., Liu, C., Xiong, J., Liu, J., Zhou, Y., 2016. A 20-year simulated climatology of global dust aerosol deposition. Sci. Total Environ. 557–558, 861–868. https://doi.org/10.1016/J.SCITOTENV.2016.03.086

Zhuang, G., Yi, Z., Duce, R., Brown, P., 1992. Link between iron and sulfur cycles suggested by Fe(II) in remote marine aerosol. Nature 355, 537–539. https://doi.org/10.1038/355537a0

Parya Broomandi: Conceptualization, Methodology, Software, Data curation, Writing- Original draft preparation.

Ferhat Karaca: Conceptualization, Methodology, Writing- Reviewing and Editing.

Mert Guney: Conceptualization, Methodology, Writing- Reviewing and Editing.

Aram Fathian: Software

Xueyu Geng: Project administration

Jong Ryeol Kim: Supervision, Project administration

Conflict of interest

The authors declare that they have no conflict of interest.

Highlights:

- Examining the seasonal variation in affected areas from sand and dust storms (SDSs) originating from war-impacted semi-arid bare lands affected by chemical warfare located in southwest Iran.
- During both cold and warm periods, Kuwait and the Persian Gulf were highly vulnerable to episodic dust incursions with locations in the maximum impact zone

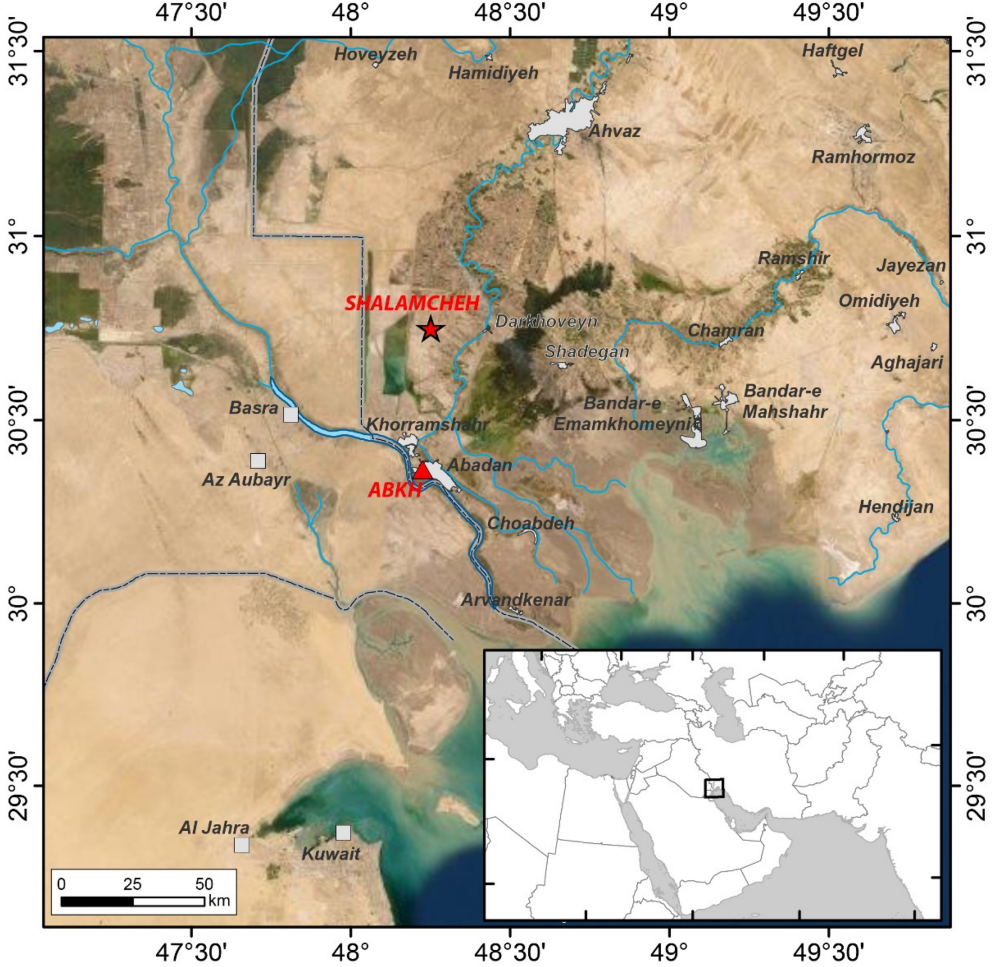
47°30'
48°
48°30'
49°
49°30'
31°30'
31°
30°30'
30°
29°30'
Hoveyzeh
Hamidiyeh
Haftgel
Ahvaz
Ramhormoz
Ramshir
Jayezan
Omidiyeh
SHALAMCHEH
Darkhoveyn
Chamran
Shadegan
Aghajari
Bandar-e
Mahshahr
Basra
Khorramshahr
Bandar-e
Emamkhomeyni
Abadan
Az Aubayr
ABKH
Hendijan
Choabdeh
Arvandkenar
Al Jahra
Kuwait
0
25
50
km

Figure 1

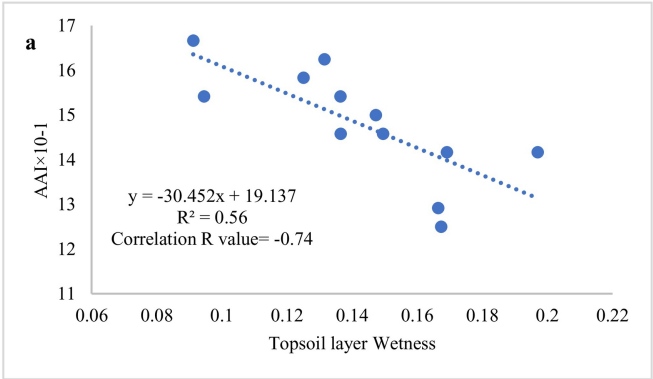
a
AAI×10-1
y = -30.452x + 19.137
R² = 0.56
Correlation R value= -0.74
Topsoil layer Wetness

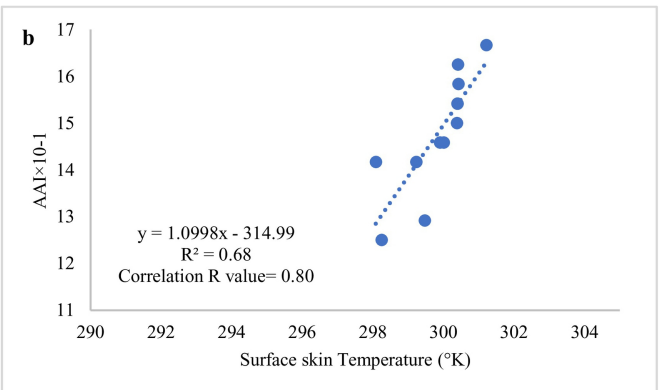
b
AAI×10-1
y = 1.0998x - 314.99
R² = 0.68
Correlation R value= 0.80
Surface skin Temperature (°K)

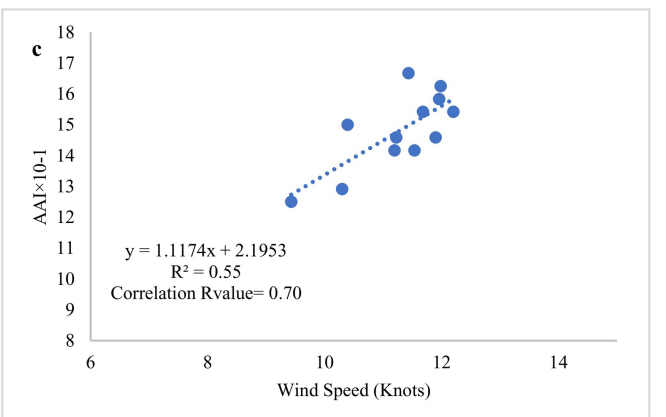
c
AAI×10-1
y = 1.1174x + 2.1953
R² = 0.55
Correlation Rvalue= 0.70
Wind Speed (Knots)

Figure 2

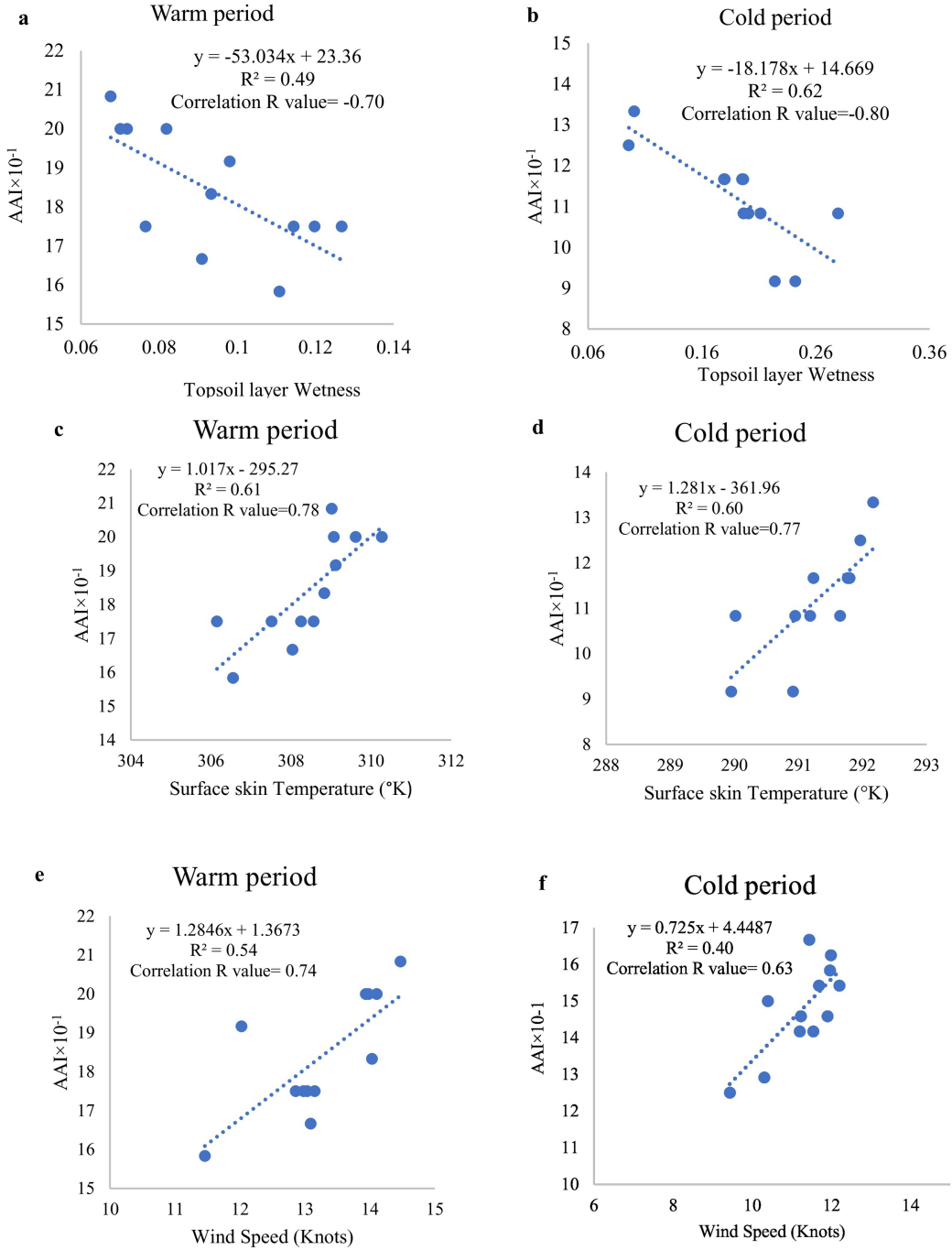
a
Warm period
y = -53.034x + 23.36
R² = 0.49
Correlation R value= -0.70
AAI×10⁻¹
Topsoil layer Wetness
b
Cold period
y = -18.178x + 14.669
R² = 0.62
Correlation R value=-0.80
AAI×10⁻¹
Topsoil layer Wetness
c
Warm period
y = 1.017x - 295.27
R² = 0.61
Correlation R value=0.78
AAI×10⁻¹
Surface skin Temperature (°K)
d
Cold period
y = 1.281x - 361.96
R² = 0.60
Correlation R value=0.77
AAI×10⁻¹
Surface skin Temperature (°K)
e
Warm period
y = 1.2846x + 1.3673
R² = 0.54
Correlation R value= 0.74
AAI×10⁻¹
Wind Speed (Knots)
f
Cold period
y = 0.725x + 4.4487
R² = 0.40
Correlation R value= 0.63
AAI×10-1
Wind Speed (Knots)

Figure 3

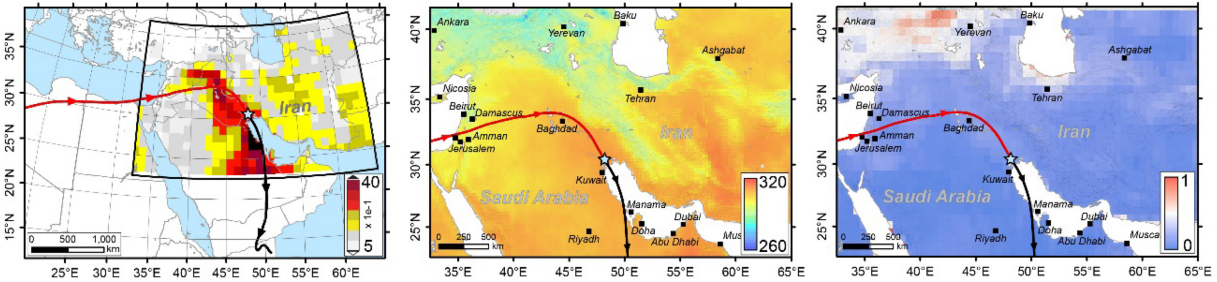

a) SDS event on 17/04/2010

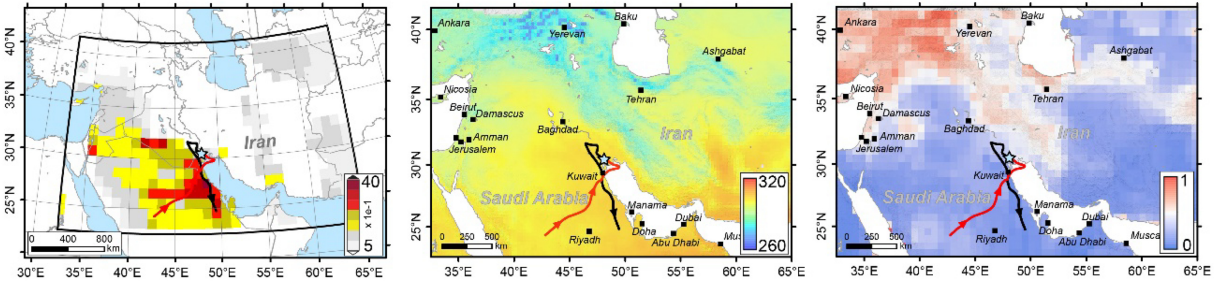

Figure 4

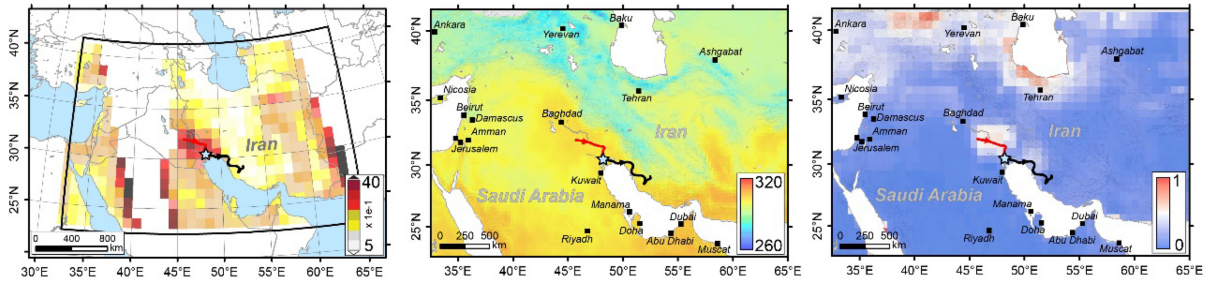

a) SDS event on 21/12/2012

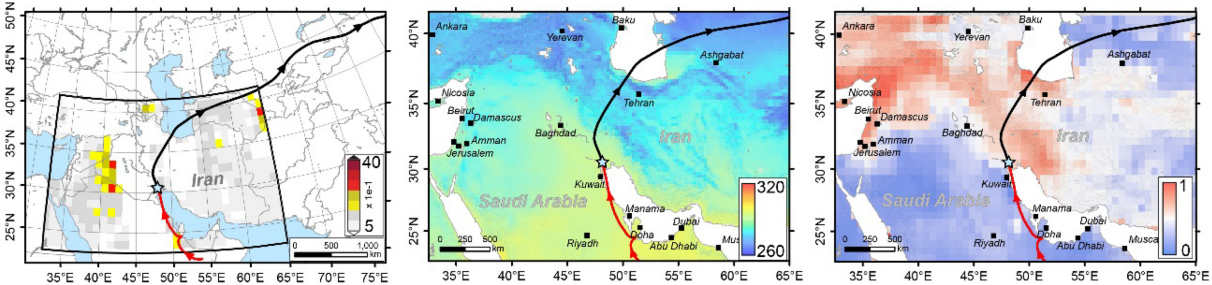

Figure 5

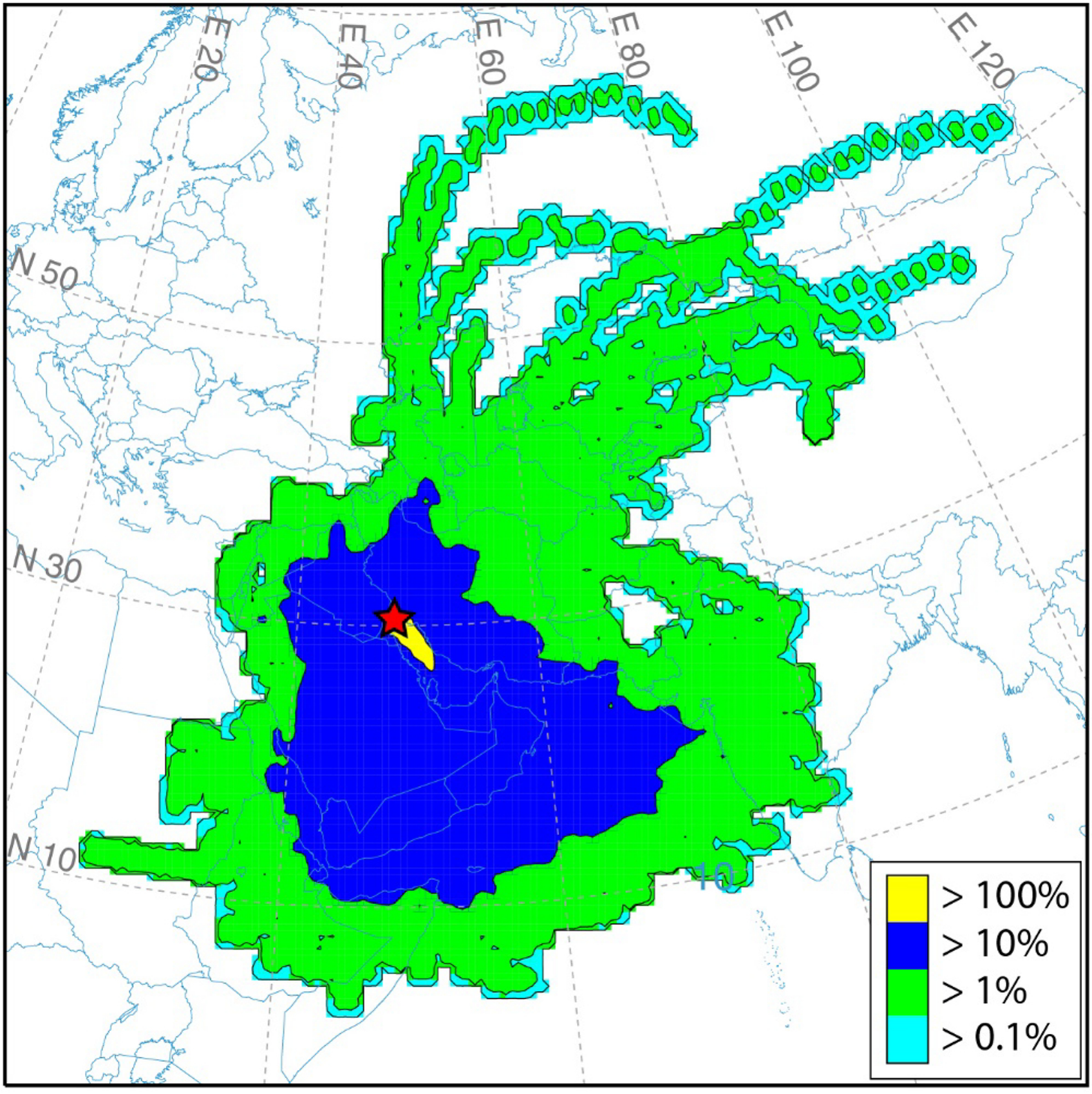

Figure 6

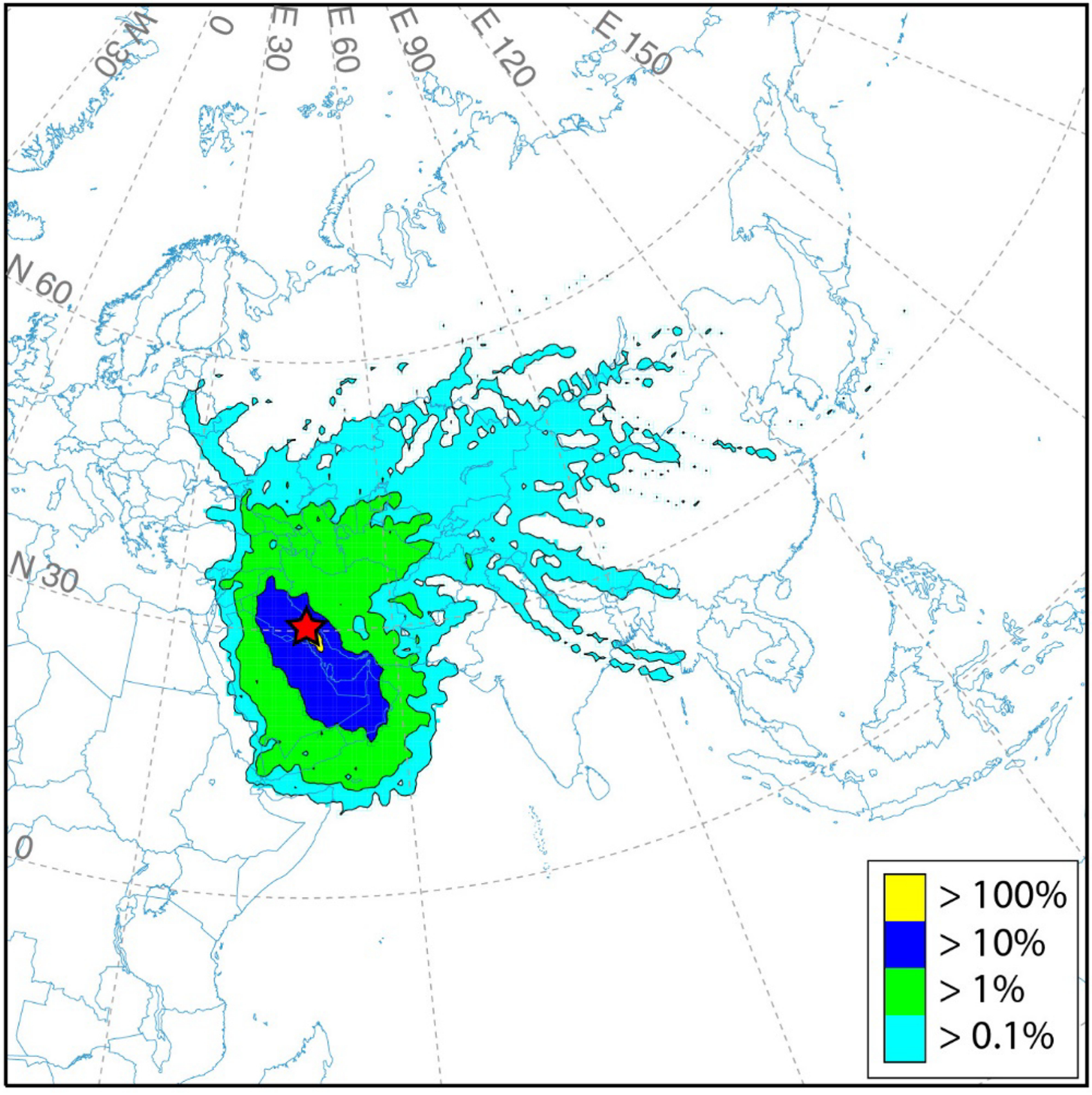

Figure 7

a) Trajectory cluster groups for warm period

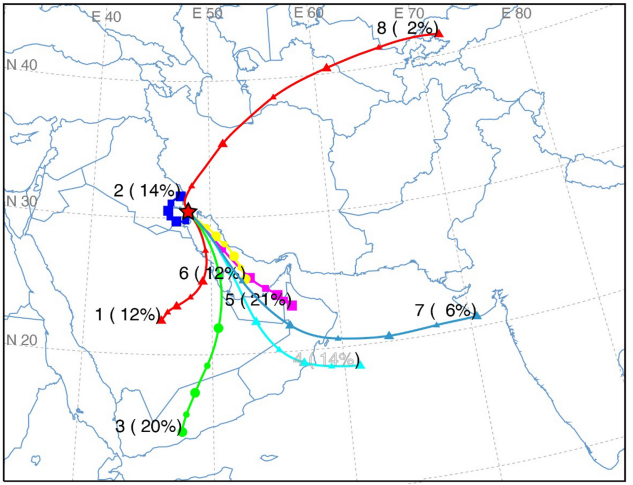

b) Trajectory cluster groups for cold period

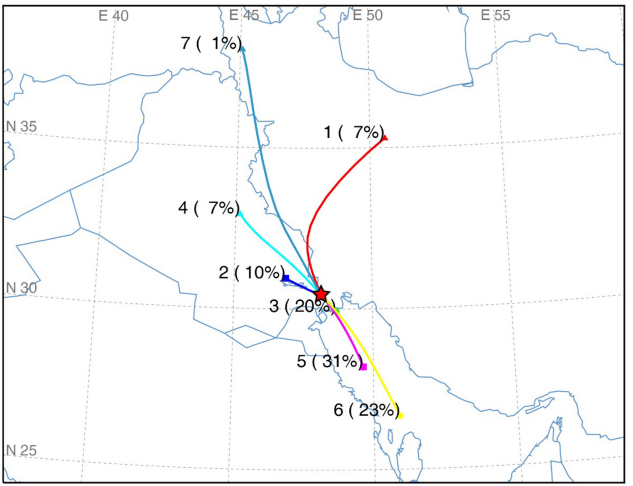

Figure 8